

**GROUND MAGNETIC AND GEOELECTRICAL PROSPECTING
FOR GOLD MINERALISATION WITHIN TSOHO- GURUSU
AREA OF MINNA, NIGER STATE, NIGERIA**

BY

**OMUGBE, Lucky Emamuro
MTech/SPS/2017/6963**

SUBMITTED

TO

**DEPARTMENT OF PHYSICS,
FEDERAL UNIVERSITY OF TECHNOLOGY, MINNA**

SEPTEMBER, 2021

**GROUND MAGNETIC AND GEOELECTRICAL PROSPECTING
FOR GOLD MINERALISATION WITHIN TSOHO- GURUSU
AREA OF MINNA, NIGER STATE, NIGERIA**

BY

**OMUGBE, Lucky Emamuro
MTech/SPS/2017/6963**

**A THESIS SUBMITTED TO THE POST GRADUATE SCHOOL, FEDERAL
UNIVERSITY OF TECHNOLOGY, MINNA, NIGER STATE, NIGERIA IN
PARTIAL FULFILLMENT OF THE REQUIREMENT FOR THE AWARD OF
THE DEGREE OF MASTER OF TECHNOLOGY IN PHYSICS (APPLIED
GEOPHYSICS)**

SEPTEMBER, 2021

ABSTRACT

Ground magnetic and geoelectrical resistivity methods were used to prospect for gold mineralisation within Tsoho-Gurusu area of Minna, Niger state. The study area is bounded with latitudes $09^{\circ} 37' 13''\text{N}$ to $09^{\circ}37'28.6''\text{N}$ and longitudes $006^{\circ} 36' 29.4''\text{E}$ to $006^{\circ} 36' 13.1''\text{E}$, with a total area of $250,000\text{ m}^2$. Magnetic was collected using Geometric 857AX proton precession magnetometer. Prior to the geophysical survey, geological mapping was conducted to map out the surface structural features. Eleven traverses were occupied and aligned in North-South direction. Each traverse is 500 m long and uniformly spaced 50 m apart. The measurement stations were position East-West, across the traverses at 10 m apart in the mineral foliation direction. The magnetic data acquired were subjected to International Geomagnetic Referenced Field to obtained the residual field. The residual field was then processed and analysed using Euler and Analytical signal methods. The Electrical Resistivity Tomography (ERT) data was collected along two profile of anomalously high residual values (-99 to 82 nT) and low TMI value. The result from the analytical signal shows both high and low amplitude anomalies with the high amplitude anomalies dominates the entire study area. The result from Euler deconvolution shows a variation of depths between 8.0 to 25.0 m. The results from the electrical resistivity method shows a depth variation between 5 – 13.4 m. Low electrical resistivity values were found to associate with the high TMI values in an East-West pattern. This anomaly pattern agreed with the major East-West and Northeast-Southwest fracture pattern captured in the rose diagram and the lineament map. These indicates that fractures are potential mineralization zones for conductive minerals. Two possible mineralised zones were identified from the study area based on 2D electrical resistivity and magnetic data. The South Eastern part along the ERT profile shows eluvial and primary gold veins. The primary veins are trending in the NE-SW in consistent with the general trend of the geological formation likewise as revealed in the ERT profile in the North Eastern part of the study area. The surface structure pattern, magnetic anomaly pattern and electrical anomaly pattern are indicative of quartz vein and eluvial deposits. Both the quartz vein and the eluvial gold deposits could be found within 5 m and 13.4 m depths.

TABLE OF CONTENTS

DECLARATION	Error! Bookmark not defined.
CERTIFICATION	Error! Bookmark not defined.
ACKNOWLEDGEMENTS	Error! Bookmark not defined.
ABSTRACT	i
LIST OF FIGURES	iv
LIST OF PLATE	vi
ABBREVIATION	vii
CHAPTER ONE	1
1.0 INTRODUCTION	1
1.1 Background to the study	1
1.2 Statement of the Research Problem	2
1.3 Aim and Objectives of the Study	4
1.4 Justification of the Study	4
1.5 Limitation of the Study	4
1.6 Location of the Study Area	5
1.7 Geological Synopsis of Niger State	5
1.8 Geology of Study Area	7
CHAPTER TWO	9
2.0 LITERATURE REVIEW	9
2.1 Review of Relevant Geophysical Work	9
2.2.1 Theoretical framework for magnetic prospecting method	13
2.2.2 Basic concepts and units of geomagnetism	14
2.2.3 Induced and remanent magnetisation	16
2.2.4 Magnetic susceptibility	17
2.2.5 Diamagnetism, paramagnetism, ferri and ferro-Magnetism	19
2.2.6 Magnetic anomalies	24
2.2.7 Magnetometers	26
2.2.8 Proton-precession magnetometer	27
2.3.1 Theoretical framework for geoelectrical prospecting methods	28
2.3.3 Basic concept of electrical resistivity method	31
2.3.4 Potential for a homogeneous medium	32
2.3.5 Electrical potential due to point current source	33

2.3.6	Electrical field survey measurements	34
2.3.7	Electrical properties of metallic and mineral ores	34
2.3.8	2-D Electrical imaging surveys (ERT)	37
CHAPTER THREE		39
3.0	MATERIALS AND METHODS	39
3.1	Materials	39
3.2	The Research Method	39
3.2.1	Field geological mapping	39
3.2.2	Acquisition of total magnetic field data by ground magnetic	40
3.2.3	Magnetic data filtering	41
3.2.4	Interpretation of magnetic anomalies	42
3.3.1	Acquisition of geoelectrical data	43
CHAPTER FOUR		46
4.0	RESULTS AND DISCUSSION	46
4.1	Results of Field Geology Mapping	46
4.2	Results of Total Magnetic Intensity Measurement	49
4.3	Result of Geoelectrical Resistivity Measurement	57
CHAPTER FIVE		59
5.0	CONCLUSION AND RECOMMENDATION	59
5.1	Conclusion	59
5.2	Recommendation	59
5.3	Contribution to Knowledge	60
	References	61

LIST OF FIGURES

1.1	Geological map of Nigeria showing Basement complex	1
1.2	Map of Study Area	5
1.3	Geological Map of Niger State	6
3.1	Earth's Magnetic Field	14
3.2	Electron Spin in Diamagnetic and Paramagnetic Materials	20
3.3	Schematic of Magnetic Moments	21
3.4	Geomagnetic Elements and Vector Representation	23
3.5	The Horizontal (ΔH), Vertical (ΔZ) and total Field (ΔB) anomalies	24
3.6	Principle of Proton-Precession Magnetometer	26
3.7	The Approximate Range of Resistivity Values of Common Rocks	28
3.8	Current Flow from Single Surface Electrode	31
3.9	The Potential Distribution Caused by a Pair of Current Electrodes	33
3.10	Basic Setup for a Resistivity Survey	34
3.11	The Resistivity of Rocks, Soil and Minerals	34
3.12	Sequence of Measurements to Build up Pseudosection	35
3.13	Flow Chart Showing the Method of Study	43
4.1	Geologic Map of the Study Area	44
4.2	Rose Diagram	46
4.3	Lineament and Profile of Ground magnetic survey	49
4.4	Total Magnetic Intensity Map	50
4.5	Total Magnetic Intensity Contour Map of the Study Area	51
4.6	Residual Map of Study Area	52
4.7	Euler Map Showing Depth to Source Body	53
4.8	Analytical Signal Map Showing Shape of Causative Body	54

4.9	2-D Resistivity Profile Section	56
4.10	2-D Resistivity Profile Section	57

LIST OF PLATE

i.	Tunneling by Artisanal Miners carried out on the Study Area	3
ii.	Pitting	3
iii.	Magnetic data Acquisition using Geometrics 857Ax Proton Precession	39
iv.	Geoelectric Data Acquisition	42
v.	Quartz Vein	45
vi.	Sets of Joints/Fracture	46

ABBREVIATION

ERT	Electrical Resistivity Tomography
TMI	Total Magnetic Intensity
Cgs	Centimeter-gram-second
TRM	Thermoremanent Magnetization
DRM	Detrital Remanent Magnetization
VRM	Viscous Remanent Magnetization
AM	Amperes Permeter
B	Flux Density
H	Magnetising Force
K	Magnetic Susceptibility
EMU	Electromagnetic Units
E	Field Intensity
J	Current Density
σ	Conductivity
ρ	Resistivity
I	Current Source
ρ_a	Apparent Resistivity
CET	Centre for Exploration Target
GPs	Geographic Position System

CHAPTER ONE

1.0 INTRODUCTION

1.1 Background to the study

The Basement Complex is a group of igneous and metamorphic rocks that range from Precambrian to Palaeozoic age in Nigeria. The major lithologic units within this complex are migmatite, gneiss, quartzite, schist, granite and acid and basic dykes (Obaje, 2009). The group of rocks are also known as massifs. They constitute the Northern Nigeria basement in North central Nigeria, the Western Nigeria basement in Western Nigeria, Adamawa Sanduana in North Eastern and Eastern Nigeria basement complex. It is these Basement complex that delimit the Nigeria sedimentary basins (Obaje, 2009).

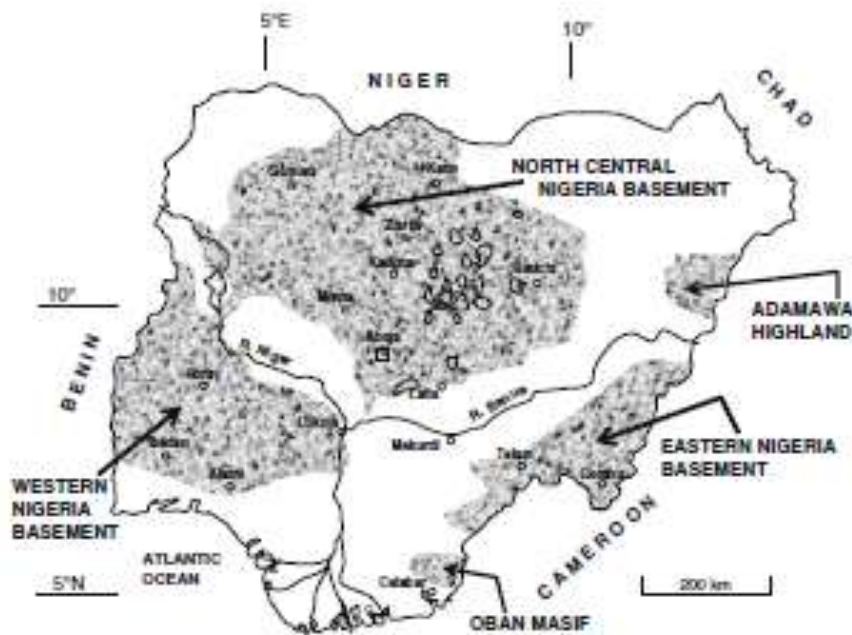


Figure 1.1: Geological map of Nigeria showing Basement complex (Obaje, 2009).

Figure 1.1 illustrates the spatial distribution of Basement rock of the Nigeria complexes. Various industrial and ore minerals are hosted within the Basement Complex rocks. One of

such ore minerals is gold. Economic gold deposits are hosted in alluvial placers, eluvial bodies and primary veins within Nigeria schist belts. Reported locations of gold ore in Northern Nigeria in Schist belts include; Anka, Bin Yauri, Gurmana, Iperindo, Malele, Maru, Okolom-Dogondaji and Tsoho Birni Gwari-Kwaga. Primary gold mineralisation is explored for within the neighbourhood of igneous intrusions. It occurs in association with pyrrhotite, magnetite and ilmenite (Mbonimpa *et al.*, 2007). These associated minerals possess high magnetic susceptibility. Consequently, the composite of these minerals and gold in rocks impart high magnetic susceptibility on the host rocks. It is this attribute of gold hosted rocks that makes the magnetic an effective tool for the prospecting for them (Fareed, 2016).

The use of magnetic methods is germane in metal ores which can be magnetic as well as electrically conductive with clear signature (Lyasky, 2010). Thus, the magnetic method is commonly employed to delineate areas with potential for gold mineralisation (Peter, 2019). High conductivity of gold makes electrical resistivity prospecting technique also effective in prospecting for them. The combinations of magnetic and electrical resistivity method do effectively delineate eluvial and primary gold ores. Co-ordinated development of delineated gold ores and associated minerals constitute a potent approach to the Nigeria mono-economy that has been hitched on petroleum exploitation for too long.

1.2 Statement of the Research Problem

For over a decade, artisanal miners have employed surface excavation and tunnelling to search for gold mineralisation in Tsoho Gurusu. This involves heavy manual labour which has been little rewarded because their effort has been based on intuition, and not on geoscience principles and geophysical information. The surface excavation and tunnelling have resulted in environmental degradation of the area (Plate I and II). The coincidence of

high total magnetic field intensity anomaly with low electrical resistivity anomaly delineates areas for mining activates from the larger barren areas, thus minimising prospecting costs and avoiding widespread environmental degradation. Such requisite geophysical information for improving miner's success and minimising environmental degradation in Tsohon Gurusu is yet to be systematically generated.



Plate I: Tunnelling by artisanal miners carried in the study area.



Plate II: Pitting

1.3 Aim and Objectives of the Study

The aim of this research is to delineate areas with potential for eluvial and primary gold ores from surface total magnetic field intensity and geoelectric resistivity tomographic data interpretation.

The objectives of the study are to:

- i. Produce geological map of Tsohon-Gurusu on the scale of 1: 25,000
- ii. Ascertain orientation pattern of the various fracture systems from surface expression and magnetic data
- iii. Produce total magnetic field intensity map as well as its residual map and
- iv. Produce spatial depth variation maps for the magnetic source and 2D geoelectric section for the area.

1.4 Justification of the Study

The result of this work will delineate potential areas with eluvial and primary gold ore deposits. This will improve miners' rewards by minimising prospecting costs. It will also minimise widespread environmental degradation as mining activities are concentrated on delineated areas rather being conducted on blind excavation and tunnelling. Successful application of combined techniques will stimulate similar application for gold prospecting within other parts of Northern Nigeria.

1.5 Limitation of the Study

The study will be limited to ground magnetic and geoelectrical investigation of 250,000 m² areal extent of Tsohon-Gurusu.

1.6 Location of the Study Area

The study area lies within latitudes $09^{\circ} 37' 13''\text{N}$ to $09^{\circ}37'28.6'' \text{N}$ and longitudes $006^{\circ} 36' 29.4'' \text{E}$ to $006^{\circ} 36' 13.1''\text{E}$ of North-Central Nigeria (Figure 1.2). It covers surface area of $250,000\text{m}^2$.

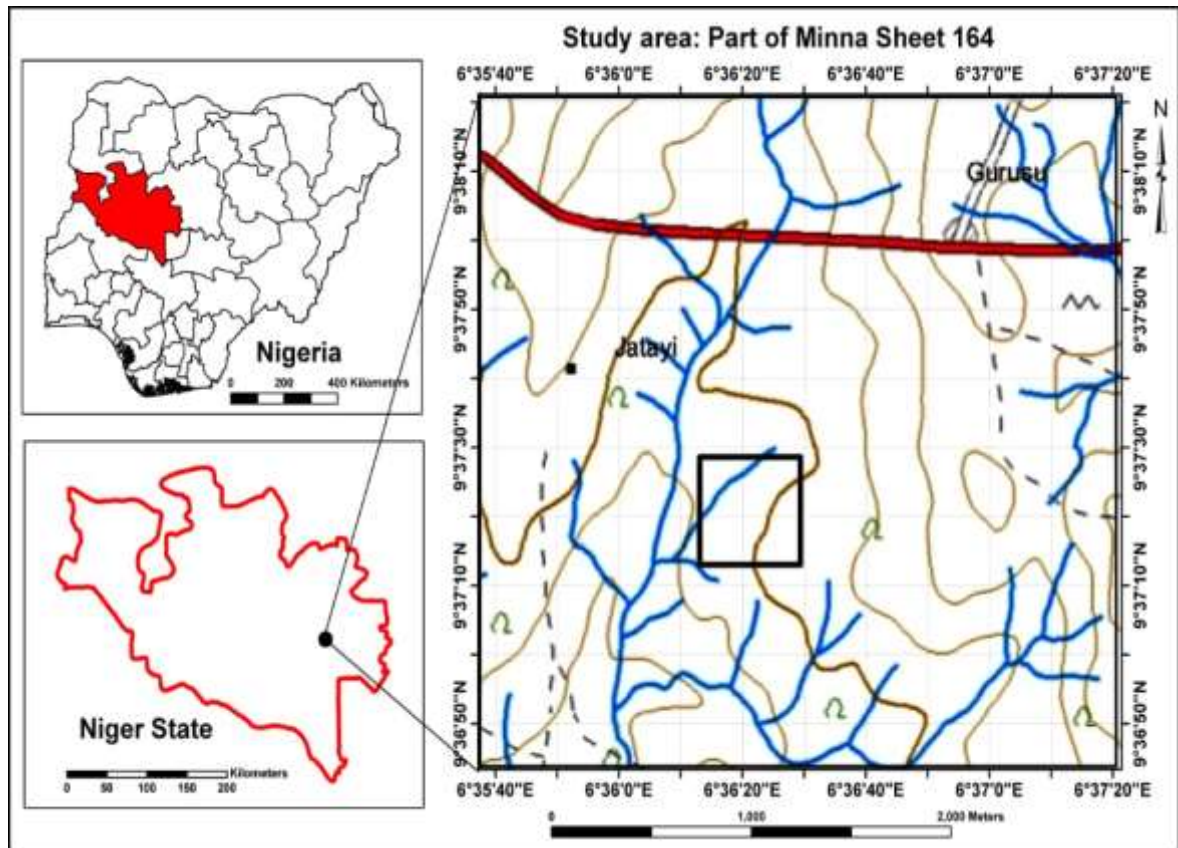


Figure 1.2: Map of the Study Area, Sheet 164 Minna Southwest.

1.7 Geological Synopsis of Niger State

About one half of the land mass of Niger State is underlain by the basement complex rocks while the other half is occupied by the Cretaceous sedimentary rocks of the Bida Basin and part of the Sokoto Basin. Figure 1.3 is the geological map of Niger State showing the lithological units as adapted from Idris-Nda (2015). Oyawoye (1972), McCurry (1989) and Ajibade (1989) described basement rocks of Precambrian gneisses, migmatites and schists

intruded by granitoids. The migmatite-gneiss complex includes migmatites, gneisses, mylonites and amphibolites. Truswell and Cope (1963) opined that the mylonites are major shear zones which mark the stratigraphic breaks between the gneissic basement complex and the cover rocks of the Birnin-Gwari Schist formation. metasedimentary

The schist belts area occurs as two elongated bodies separated by the older granite suite. The tips of the two formations are separated by a 40 km expanse of the Older Granite suite (Ajibade *et al.*, 2008). However, this study indicates a much smaller separation of less than 10 km. The Birnin-Gwari formation lies to the west of the older granite (the Minna Batholith) while the Kushaka formation lies to the East.

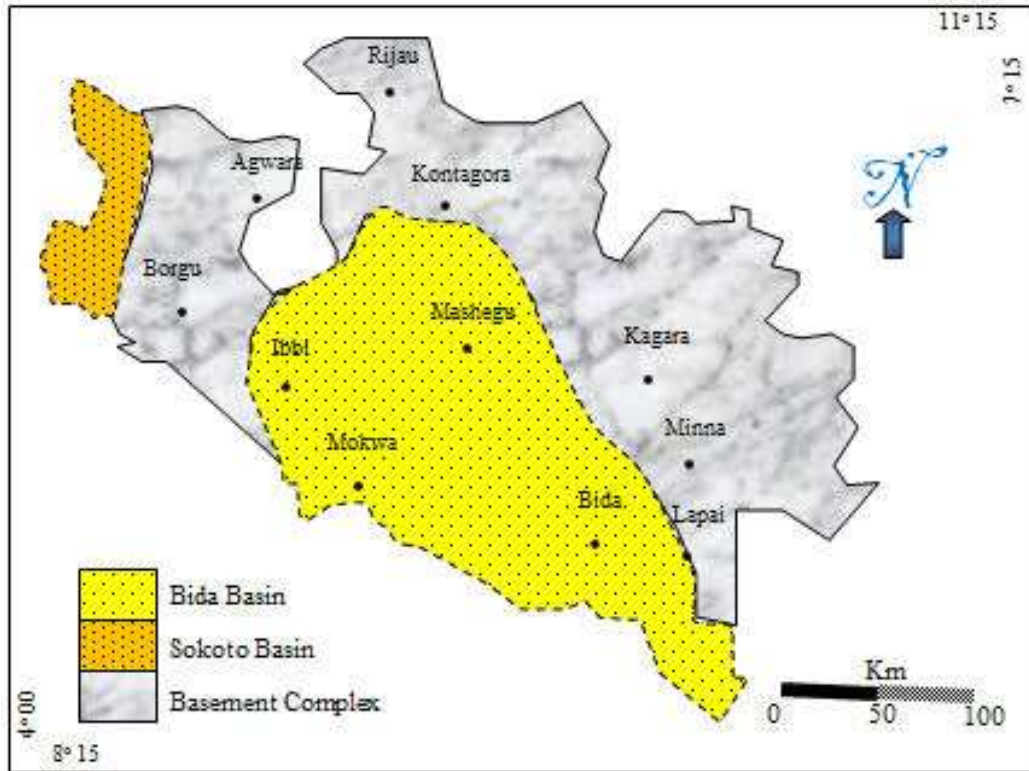


Figure 1.3: Geological map of Niger State (Adapted after Idris-Nda, 2015)

1.8 Geology of Study Area

Tsohon Gurusu area belongs to the part of Nigeria Basement Complex called North Central Basement (Obaje, 2009) The lithological units in this area are Schist, Older granite suites and quartzites. It lies within the Kushaka Schist belt and its main rock type is semi-pelitic biotite - muscovite schist, which occasionally garnet and staurolite. Other rocks are phyllites, metasilstones and graphitic schists. Several thick units of banded garnetgrunerite iron formation are interbedded with the schists.

The schist in the area is commonly intruded by quartzites which are mostly iron-stained on weathered surfaces and along joints. The quartzites are fine grained and represent original siltstone or sandstone often of high ferruginous origin.

In Nigeria, the primary veins and eluvial gold deposit appears to be Orogenic type which is controlled by deep seated curvilinear trans-crustal fracture system (Haruna, 2017). These deep-seated fracture systems are believed to serve as conduits for the subsidiary fractures which are linked to these major fracture and forms sites for gold depositions which is the main source of gold for humanity. During Orogenesis, basic and acid igneous rocks are formed and subsequently acted upon by tectonic activities that lead to deformation and metamorphism during this episode (Abubakar, 2012). Most ore deposits are hosted by metamorphic rocks and metamorphic fluids serve as basic source for various deposits (Bruce *et al.*, 2013).

CHAPTER TWO

2.0 LITERATURE REVIEW

2.1 Review of Relevant Geophysical Work

Geophysical tools for mineral prospecting in basement environment provide information on lithologic, metamorphic and structural features which can host variety of mineral deposit and generate very complex patterns of geophysical anomalies, Sultan *et al.* (2009) researched on exploration for gold and associated minerals using more than one geophysical method to evaluate ore mineral deposit in Wadi El Beida, South Eastern desert, Egypt, They employed Magnetic and geoelectrical methods to delineate the mineral ore deposits in terms of depths and extension through the structural shearing zones.

Bernard *et al.* (2012) employed magnetic and electrical technique as follow-up to show the complicated nature of ore bodies with depth and along strike. Based on the promising results from the magnetic surveys, induced polarisation (IP) surveys were completed across all the six Lady 'A' Claims in Concession. The gradient array results show south-east/north-west trending zones of high chargeability accompanied by low resistivity. There is a zone towards the eastern end of the blocks, which show high resistivity and high chargeability. High chargeability zones can be thought to correspond to zones associated with quartz veins. Real Section Induced Polarisation (RSIP) was carried out to determine the apparent behaviour of the anomalies with depth. The results from this survey showed the complicated nature of the ore-body with depth and along strike.

With the increasing demand for potable save drinking water for the populace necessitated investigating the trend of contamination from indiscriminate waste disposal associated to ground water using geoelectrical method, Rafiu and Abu (2014). The acquired data were

plotted as pseudo-resistivity sections so as to reveal the spatial distribution of contaminate plumes. Thus establishing the contamination plumes as low resistivity while areas with less vulnerability have high resistivity hence physio-chemical analysis reveals actual state of groundwater.

Tigistu *et al.* (2014) evaluate the competence of near surface formation for engineering facilities deploying the 2D electrical resistivity tomography and magnetic surveying. The study was able to identify weak zones that need special designs to mitigating against any form of occurring hazards.

Saeed *et al.* (2014) posited on geological structures are critically important in the understanding of geologic history as related to mineral prospecting which are structurally controlled. To this end, establishing the strike and trend of mineralisation in Halab Dandi, Zanjan (Iran), used magnetic and 2D electrical profiling method in exploration geophysics which happens to be an efficient method in prospecting for Sulphide mineral deposits.

The characterisation of banded iron formation deposits was accomplished with the use of multiple geophysical techniques, Kayode *et al.* (2016) which entails the usage of Aeromagnetic and Electrical methods to show that the iron ore mineralisation is associated with granite gneiss at shallow depths that are favourable for exploitation. The numbers of the varying trend of delineated structure suggest that the area has undergone more than one episode of tectonic activity which left an inprint of fracturing and faulting.

The correlation of Magnetic and ERT anomalies with lithology is germane in mineral prospecting and exploration as observed by Kheiralla *et al.* (2015), the main objective of this study is to delineate the various structural aspects in the area in addition to pilot prospecting work to pin point the gold deposits which could be related to mineralization zones. The gold

and disseminated sulfides are located on the alteration shear zone which is composed of granitic and dioritic highly ferruginated rock occupying the southwestern and central parts of the area.

The modelling of iron ore deposits was carried out by Adree and Dedi (2016). Geoelectrical resistivity method was deployed using the dipole-dipole array. A three layer geoelectric sections was established from the the 2dsection. The iron ore mineral associated with quartzite was observed from the cross section at 30 m depth from the surface.

Sedara *et al.* (2016) uses response of high and low magnetic intensities to strongly suggest the presence of ferromagnetic mineral around Ipetumodu, Southwest Nigeria. The highly mineralized regions of the study area were established. Hence, there is a need for further study using other geophysical techniques so that ground magnetic study can equally expose lithological units in basement structures to meet the demands of searching for mineral deposits in an area. Alile *et al.* (2017) carried out a 2D and 3D electrical resistivity tomography in delineating mineral deposits. The study showed that 3D geoelectrical resistivity survey can be effectively and efficiently conducted by collating apparent resistivity data from parallel and orthogonal 2D profiles. The generation of 3D data set by collating orthogonal or parallel set of 2D lines speeds up field procedure and considerably reduced the effort and cost involved in collecting 3D data set using square or rectangular grid method. The technique of collating parallel or orthogonal 2D profiles to build 3D data set has an additional advantage of producing stand-alone 2D inversion images which can be very useful in the interpretation of 3D images commonly presented as horizontal depth slices. 3-D Isocores depth and the subsurface volume were realized in the study. Abdullahi and Alabi (2018), proffer that geophysical exploration for solid mineral resources is largely dependent

on the resource, hosting geologic environment associated with its physical or chemical property which differs significantly from those of the adjacent crust.

Establishing the trend of mineralization in Kwakuti part of Niger State, Ejepu *et al.* (2018) carried out an integrated prospecting for gold mineralisation using aeromagnetic and aeroradiometric dataset for structural interpretation of the area through mapping the lithology, geologic structures, lineaments and hydrothermal alteration zones associated with gold and associated mineralisation.

Joshua *et al.*, (2017) plotted residual anomalies against distance using Microsoft excel and analytical signal was used to estimate depth of magnetic source bodies. The source bodies is established at 1 m and 13 m respectively. These magnetic source bodies is suspected to be magnetic minerals hence further improved analysis of magnetic anomaly map be done.

Adetona *et al.* (2018) was able to delineate lineaments within major structures around Eastern part of lower Benue trough from 2009 Aeromagnetic data, establishing **two** lithology with the aid of Euler deconvolution, Analytical signal and Centre for Exploration target (CET) techniques. The depth estimation of magnetic source bodies, trends of magnetic body, structural trends and establishment of contact between basement and sedimentary formation were achieved.

It identified three main structures that points at the mechanisms that is associated with the depression which allows accumulation of sediments that led to the formation of both the Anambra and Lower Benue trough. These structures are NE – SW (at the upper part of the study area) and E – W (at the lower part of the study area). A major vertically fault line that structurally define the course of river Niger within the study area, and the extension of Chain's fault line that cuts the South East corner of the study area. Also, corroborating the

existence of intrusive structures of Basaltic rocks within the lower portion of the study area that was revealed by Analytical Signal and CET grid analysis.

Ravindran (2012) uses 2D electrical imaging in the evaluation of Iron ore deposits based on the high conductivity recorded. The interpretation and analysis with regards to location premise on proximity to equator or poles requires careful analysis of magnetic data which can give vital information about zones of magnetic mineralization. Structural features such as fault, joint and fractures that host mineralization were delineated and analysed to reveal the mineralisation zones using an integrated geophysical approach (Oluwaseun *et al.*, 2014; Andrew *et al.*, 2018).

Mosaad *et al.* (2020) acquired resistivity and induced polarization data sets using the Iris El-Rec pro system with pole-dipole electrode array to characterise the sulphide ore mineralisation. It was able to characterised them into moderate resistivity values and moderate to low chargeability values.

Rowland and Ahmed (2019) revealed the deep and shallow magnetic anomaly sources for hydrocarbon potential. This is achieved through the interpretation of high resolution aeromagnetic data. The deep source anomalies vary from 2 km and 5 km while shallow source bodies have an average depth of 0.21 km. The deeper source lies around the central and south-western parts and are probable site for hydrocarbon exploitation.

2.2.1 Theoretical framework for magnetic prospecting method

Ground magnetic surveying is a passive geophysical method based on the measurement of localized disturbances and variations to the magnetic properties of rock-forming minerals. It has been the oldest geophysical method. Magnetic measurements are made more easily and

cheaply than most geophysical measurements. The magnetic field perturbation is often diagnostic of mineral structure as well as regional structure and is the most versatile of geophysical prospecting techniques (Telford *et al.*, 1990).

Magnetic methods can be used in a wide variety of applications and ranges from small-scale investigations in the mapping of sedimentary thickness, archaeological remains, mapping of salt dunes, basic igneous dykes, geological boundaries between magnetically contrasting lithology including faults and through to large-scale regional geological mapping to determine gross structure as in hydrocarbon exploration (Reynolds, 2011).

2.2.2 Basic concepts and units of geomagnetism

The earth's magnetic flux is believed to originate from liquid iron in the earth outer core as a result of subsurface convectional activities (Nabighian *et al.*, 2005). The magnetic flux is often described by magnetic lines of force that are invisible. These lines are often thought of as flowing out of the south magnetic pole and into the north magnetic pole. A compass needle aligns itself along the magnetic line of force that passes through it. If the compass needle were free to move vertically as well as horizontally, it would point vertically downward at the north magnetic pole, vertically upward at the south magnetic pole and at intermediate angles away from the magnetic poles. Figure 2.1 illustrates the Earth's Magnetic field. Within the Earth magnetic field, a magnetic flux exists, as indicated by the flux lines and converges near the ends of the magnet, which are known as the magnetic poles. Assuming a bar magnet, if such magnet is suspended in free air, the magnet will align itself with the Earth's magnetic field with one pole (the positive north-seeking) pointing towards the Earth North Pole and the other (the negative south-seeking) towards the south magnetic pole (Philip *et al.*, 2002). Magnetic poles always exist in pairs of opposite sense to form a dipole and the single pole is referred to as a monopole.

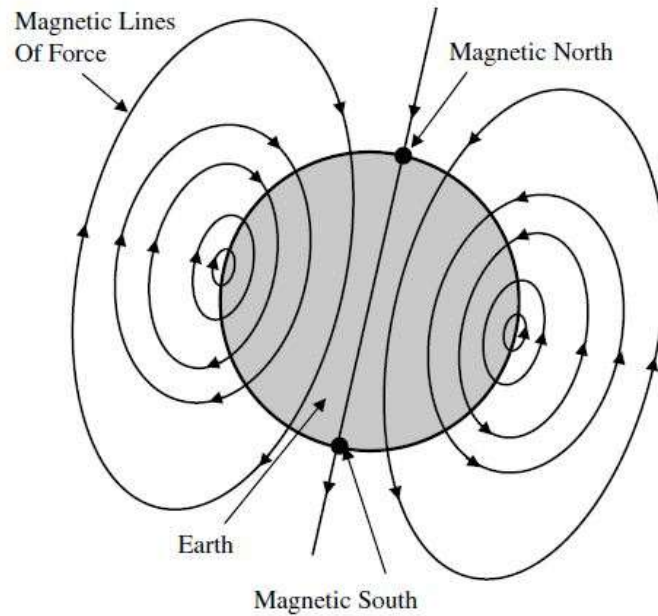


Figure 2.1: Earth's magnetic field

If two magnetic poles of strength m_1 and m_2 are separated by a distance r , μ_0 and μ_R are permeability of vacuum and relative permeability of medium, a force exists between them is given as;

$$\mathbf{F} = \frac{\mu_0 m_1 m_2}{4\pi \mu_R r^2} \quad 2.1$$

If the poles are of the same sort, the force will push the poles apart, and if they are of opposite polarity, the force is attractive and will draw the poles towards each other. The closeness of the flux per unit area, is the flux density \mathbf{B} (and is measured in weber/m² = Tesla). \mathbf{B} , which is also called the 'magnetic induction', is a vector quantity (the former centimeter-gram-second (c.g.s.) units of flux density were gauss, equivalent to 10⁻⁴ T.) The units of tesla are too large so a subunit called the nanotesla (nT = 10⁻⁹ T).

The Earth's magnetic intensity is in the range of 25,000-70,000 nT, except for small levels of perturbations to the field intensity. The sought-after field precision is usually 1 γ , or 10^{-5} of total field intensity of the earth. However, anomalies can result in few 100 γ amplitudes.

2.2.3 Induced and remanent magnetisation

The phenomenon that described the tendency of a material that loses its magnetisation acquired in the direction of the field when it is removed from that field is known as induced magnetisation. While the inherited magnetisation left after the removal of the applied field is the remanent magnetisation. It is the actual magnetic properties that are embedded in the rock during its emplacement or formation. In many cases, the magnetisation of rocks depends on the present geomagnetic field and the magnetic mineral content (Telford *et al.*, 1990).

The remanent or permanent magnetisation could take the form of primary remanent or secondary remanent magnetisation. Primary remanent magnetisation can be acquired either as the igneous rock solidifies and cools through the Curie temperature of its magnetic minerals often refers to as Thermoremanent magnetisation (TRM) or as sedimentation of magnetic particles within the sediment aligns themselves with the earth field often refers to as Detrital remanent magnetisation (DRM). The secondary remanent magnetisation occurs as magnetic mineral recrystallisation takes place or grows during diagenesis or metamorphism, Chemical remanent magnetisation is thus achieved. When they develop slowly in an ambient magnetic field, the magnetic mineral aligns in the direction of earth field known as viscous remanent magnetisation (VRM).

The amount of induced or remanent magnetisation in an object is called its magnetic moment. This property can be quantified with the unit ampere-meter-squared, Am^2 . For objects that are weakly magnetic, a unit that is 1000 times smaller may be applied; this is called the milliamperere meter-squared, mAm^2 . These units quantify the total amount of magnetic

material in an object. The same unit is applied to induced and remanent magnetisation; the sum of these two quantities is called total magnetisation. In order to compare these quantities from one material to the next, one can divide each magnetic moment by the mass or the volume of that object; these values might be called relative magnetic moments. However, when the magnetic moment of an object is divided by its volume, the result is called the intensity of magnetisation of the object; this has the unit of Amperes per meter, A/m.

When the remanent magnetization of an object is divided by its induced magnetization, the result is called the Q ratio (sometimes referred to as the Königsberger ratio).

$$Q = J_r / k (F / \mu_0) \quad 2.2$$

where J_r is the intensity of remanent magnetisation, k is the susceptibility, μ_0 is the permeability of free space and F is the magnitude of the Earth's magnetic field (in tesla) at a given location in the same sense as the B-field (flux density).

2.2.4 Magnetic susceptibility

Rock forming minerals exhibit an inherent property to be magnetised in the presence of an applied magnetic field. This phenomenon is true for most rock forming minerals or rock units except for permanent magnets. It is possible to express the relationship between B and H in terms of a geologically diagnostic parameter, the magnetic susceptibility K. Susceptibility is in essence a degree of how susceptible a material is to becoming magnetised (Reynolds, 2011). For a vacuum, $\mu_r = 1$ and $k = 0$. Although susceptibility has no units, to rationalise its numerical value to be compatible with the SI or rationalised system of units, the value in c.g.s. equivalent units (e.g. unrationalised units such as e.m.u., electromagnetic units) should be multiplied by 4π . Relationship between magnetic flux density B, magnetising force H, and susceptibility k.

Given:

$$\mathbf{B} = \mu \mathbf{H} \quad 2.3$$

[units: μ (Wb/Am). \mathbf{H} (A/m) = W b/m²= tesla]

Since $\mu = \mu_r \mu_o$

$$\mathbf{B} = \mu_r \mu_o \mathbf{H} \quad 2.4$$

Rearranging to introduce $k = \mu_r - 1$

$$\mathbf{B} = \mu_o \mathbf{H} + \mu_o (\mu_r - 1) \mathbf{H} \quad 2.5$$

$$= \mu_o \mathbf{H} + \mu_o k \mathbf{H}$$

$$= \mu_o \mathbf{H} + \mu_o \mathbf{J} \quad 2.6$$

Hence

$$\mathbf{B} = \mu_o \mathbf{H} (1+k) \quad 2.7$$

$$\text{And } \mathbf{J} = k \mathbf{H} \quad 2.8$$

Magnetic susceptibility is an extremely important property of rocks. Rocks that have a significant concentration of ferromagnetic or ferrimagnetic minerals tend to have the highest susceptibilities. Consequently, basic and ultrabasic rocks have the highest susceptibilities, acidic igneous and metamorphic rocks have intermediate to low values, though some materials have negative magnetic susceptibility as could be seen in the susceptibility Table 2.1.

Susceptibility depends on the magnetic mineral characteristics in the rock, for a vacuum $\mu_r = 1$ and $k = 0$; where μ_r is the relative permeability (Philip *et al.*, 2002). The susceptibility of a rock-forming mineral depends largely on composition, structure and percentage volume of magnetic minerals. It is also dependent on the state of magnetization and grain size.

The magnitude of susceptibility found in common rocks and minerals are of variable orders. Highest susceptibilities are basically associated with basic igneous rock type, which explains its high constituent of magnetite. With increasing acidity of the rock constituent, the proportion of magnetite also decreases with a low susceptibility, k . An example is fresh granite. Metamorphic rock unit has its susceptibility closely associated with the availability and abundance of oxides (O_2) at the time of its formation. Rocks of sedimentary origin usually exhibit a very low susceptibility and as such structures related to sedimentary units rarely exhibit large magnetic anomalies. However, an igneous body intruding into sedimentary environment at near surface or deep seated, will give rise to a magnetic anomaly of high order of susceptibility. Notable causes of such magnetic anomalies are subsurface geological structures. Embedded in it are ore bodies that contain magnetite that generate magnetic anomalies of large-amplitude. Magnetic anomalies can be used to detect the thickness of sedimentary basins in ascertaining hydrocarbon generation and depth to basement rock.

2.2.5 Diamagnetism, paramagnetism, ferri and ferro-Magnetism

All atoms have a magnetic moment as a result of the orbital motion of electrons around the nucleus and the spin of the electrons. According to quantum theory, two electrons can exist in the same electron shell (or state) as long as they spin in opposite direction that is spin up or spin down. An electron is a moving charge and a moving charge produces a magnetic field- electron is considered as a tiny magnet. A situation where one electron spin up and other spin down, the magnetic moments of two such electrons (figure 2.2), called paired electrons, will cancel out. This situation is called Diamagnetism. In the majority of substances, when there is no external applied magnetic field, the spin magnetic moments of

Table 2.1 Susceptibilities of rocks and minerals (Reynolds, 2011)

Mineral Or Rock Type	Susceptibility (dimensionless)
Metamorphic	
Schist	315 to 3,000
Gneiss	125 to 25,000
Average for various	0 to 73,000
Igneous	
Granite	10 to 65
Granite(m)	20 to 50,000
Minerals	
Quartz(d)	-15
Pyrite(o)	50 to 5,000
Hematite(o)	420 to 38,000
Pyrrhotite(o)	1250 to 6.3×10^6
Magnetite(o)	70, 000 to 2×10^7

(d) -diamagnetic materials; (o) –Ore; (m) – with magnetic materials

$k \times 10^6$ rationalised SIunits; to convert to the unrationalised c.g.s units divide by 4π

adjacent atoms are distributed randomly, so there is no overall magnetisation. The electrons orbit in such a way so as to produce a magnetic field that opposes the applied field, giving rise to a weak, negative susceptibility examples are halite and quartz.

In a paramagnetic material the two unpaired electrons with parallel spin the magnetic field of the electrons are together. In this case the incomplete electron shells produce unbalanced spin magnetic moments and weak magnetic interactions, between atom such as fayelite, amphiboles, pyroxenes, olivine, garnets and biotite. When places in an external field, the magnetic moments align themselves into the same direction, although this process is retarded by thermal agitation. The result is a weak positive susceptibility which decreases inversely with the absolute temperature. However, it is generally in the order of magnitude stronger than diamagnetic materials.

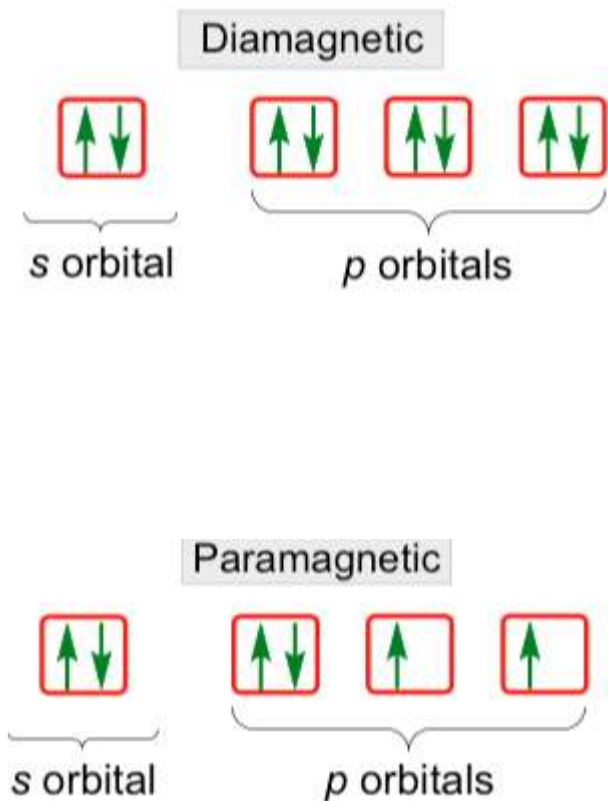


Figure 2.2: Electron spin in Diamagnetic and Paramagnetic materials

When the atomic magnetic moments of an atom arrange in a lattice can interact to align parallel to each other is referred to as ferromagnetic material (Figure 2.3A), and when they are anti-parallel to each other it is anti-ferromagnetic material (Figure 2.3B). The spin magnetic moments of the unpaired electrons are coupled magnetically due to strong interaction that exist between adjacent atoms and overlap electrons within domain and outside the domain. The small grain within which the magnetic couplings exist is called a single magnetic domain. As the electron tends to interact they are laid in response to the inducing magnetic field and retain such orientation when the inducing field is removed. This is mainly peculiar with Iron, Cobalt and Nickel.

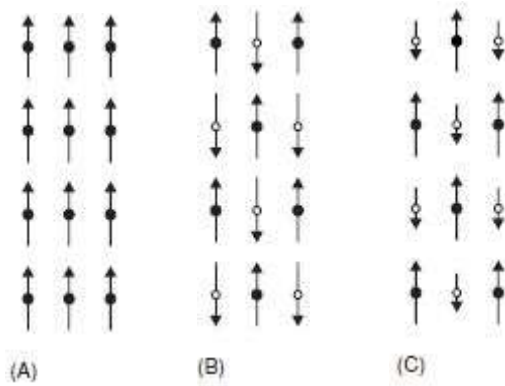


Figure 2.3: Schematic of magnetic moments in (A) ferromagnetic, (B) anti-ferromagnetic and (C) ferrimagnetic crystals. After (Reynolds, 2011).

Ferromagnetism decreases with increasing temperature and disappears completely at the Curie temperature. The Curie temperature is the point at which magnetic materials loses its magnetic characteristics. However, ferromagnetic minerals do not exist in nature. Domains in some materials are subdivided into subdomains that align in opposite directions in that their moments almost cancel out each other, though could be considered as ferromagnetic but their susceptibility is quite low. This is referred to as anti-ferromagnetic material and example is the hematite.

The magnetic subdomain of ferromagnetic materials as seen in Figure 2.3C aligns in opposition but their net magnetic moment is not zero which mainly attributed to the strength of magnetic alignment and dominant subdomain. Example of one type is magnetite and titanomagnetite, oxides of Iron and Iron of titanium. Pyrrhotite is the second type. All magnetic minerals are ferromagnetic (Telford *et al.*, 1990).

In ferromagnetic materials such as magnetite, the dipole coupling is similarly antiparallel, but the strength of dipoles in each direction are unequal (Philip *et al.*, 2002). As a result, they exhibit a strong spontaneous magnetization and susceptibility hence all minerals responsibly for magnetic property of common rock types fall into this category.

2.2.6 Magnetic anomalies

The shapes of magnetic anomalies are related to geomagnetic field and thus the directions are with respect to magnetic north (H): Total magnetic field vector (B) has a vertical component in the z-axis and is positive downwards and we assume all locations are in the northern hemisphere (Telford *et al.*, 1990). Figure 2.4 used vector diagram in the description of the normal geomagnetic field, it recognises that geomagnetic elements are related by B, H and Z which are respectively total field vector, horizontal and vector components, by;

$$B^2 = H^2 + Z^2 \quad 2.9$$

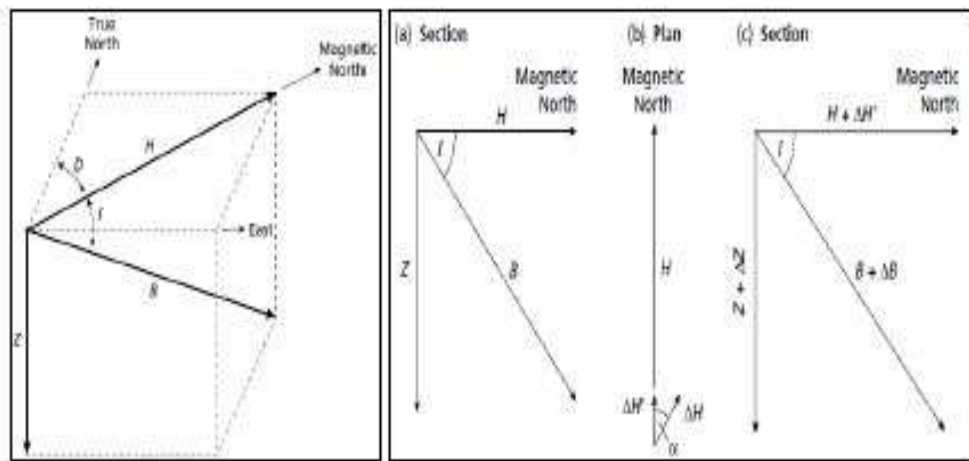


Figure 2.4: Geomagnetic elements and vector representation of the geomagnetic field with or without a superimposed magnetic anomaly (Philip *et al.*, 2002).

If an anomaly is superimposed on the geomagnetic field, it causes a change ΔB in the strength of field vector, B. Similarly, H changes by ΔH , and Z by ΔZ so that equation (2.9) becomes

$$(B + \Delta B)^2 = (\Delta H + H)^2 + (\Delta Z + Z)^2 \quad 2.10$$

Thus an anomaly produces a component in the vertical direction ΔZ and α at angle to the horizontal direction H. Where α is an angle to H (Figure 2.4b) it is only that part of ΔH in the direction of H, given as $\Delta H'$ that would contribute to the anomaly, (Philip *et al.*, 2002). Hence equation now becomes

$$\Delta H' = \Delta H \cos \alpha \quad 2.11$$

Using similar vector diagram to include the magnetic anomaly in figure 2.4c

$$(B + \Delta B)^2 = (H + \Delta H')^2 + (Z + \Delta Z)^2$$

Expanding the above equation, the equality of equation 2.9 substituted it becomes

$$\Delta B = \Delta Z \frac{Z}{B} + \Delta H' \frac{H}{B} \quad 2.12$$

Substituting equation 2.9 and angular description of geomagnetic element ratios gives

$$\Delta B = \Delta Z \sin I + \Delta H \cos I \cos \alpha \quad 2.13$$

Where I is the inclination of the geomagnetic field

Philip *et al.*, 2002 used this approach to calculate the magnetic anomaly caused by a small isolated magnetic pole of strength m, as an effect of the positive observation point situated at depth z, a horizontal distance of x and radial distance r as seen in figure 2.5. The force of repulsion on the unit positive pole ΔB_r in the direction of r is given by substitution in equation (2.1), with $\mu_R = 1$

$$\Delta B_r = \frac{Cm}{r^2} \quad 2.14$$

$$\text{Where } C = \frac{\mu_0}{4\pi} \quad 2.15$$

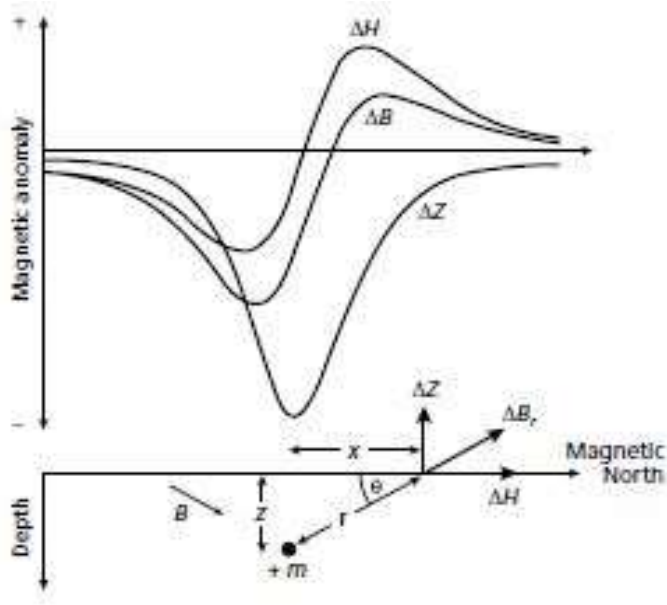


Figure 2.5: The horizontal (ΔH), vertical (ΔZ) and total field (ΔB) anomalies due to an isolated positive pole (Philip *et al.*, 2002).

The horizontal component (ΔH) and vertical (ΔZ) components of this force can be computed by resolving the appropriate directions;

$$\Delta H = \frac{C_m}{r^2} \cos\theta = \frac{C_{mx}}{r^3} \quad 2.16$$

$$\Delta Z = \frac{-C_m}{r^2} \sin\theta = \frac{-C_{mz}}{r^3} \quad 2.17$$

The z-axis is positive downward but by convention it is negative. Plots of the form of anomalies are shown on figure 2.4

2.2.7 Magnetometers

The instrument used to measure magnetic field is called magnetometers. Hitherto 1940s, they were mechanical instruments and were cumbersome, delicate and slow to operate hence were designed to measure changes in a selected components of the magnetic field most commonly the vertical field. These types have been surpassed by the more sensitive, robust electronic instruments. The important ones include; flux gate, proton-precession and optically pumped magnetometers.

2.2.8 Proton-precession magnetometer

The basic working principle of a Proton-Precession magnetometer as shown in figure 2.6 consist of a direct current flowing in a solenoid that creates a strong magnetic field around a hydrogen rich fluid usually a bottle containing some 200 –500 cc proton rich liquid such as water (good but not practical in cold climate), alcohol or kerosene. Around the bottle there are about 1000 windings of copper or aluminum wire for applying a polarizing field to the liquid (fields up to 0.01 T are used) and for picking up the signal from the processing protons after cutting off the polarizing field. In the measurement the bottle is oriented so that the polarizing field is roughly perpendicular to the measured field. When the polarizing field is cut off rapidly, the protons begin to process around the magnetic field vector (at an angular velocity ω known as Larmor precession frequency), whose magnitude is to be measured. The signal from the protons is small, only of the order of one microvolt in the coil, but its frequency is measurable for 1 – 5 seconds depending on the homogeneity of the measured field and the polarizing field used. The relationship between the frequency of the induced current and the strength of the magnetic field is called the proton gyromagnetic ratio γ .

$$\omega=2\pi f=\gamma B \quad 2.18$$

$$\rightarrow B=2\pi f/\gamma=g f, \quad 2.19$$

$$\text{Where } g=2\pi/\gamma=23.487 \text{ nT/Hz} \quad 2.20$$

The polarization of the liquid in the sensor bottle takes, depending on the field used, usually 2 – 6 seconds. The longer times are used for getting more protons oriented into the direction of the field, which means a stronger and longer signal in the measurement, allowing higher sensitivity (0.1 nT) to be used. The proton –precession magnetometer has essential no mechanical parts although the electronic components are relatively complex with a high

sensitivity approximately 1nT that is essentially drift free, it requires no orientation or leveling and measures the strength of the field but not its direction.

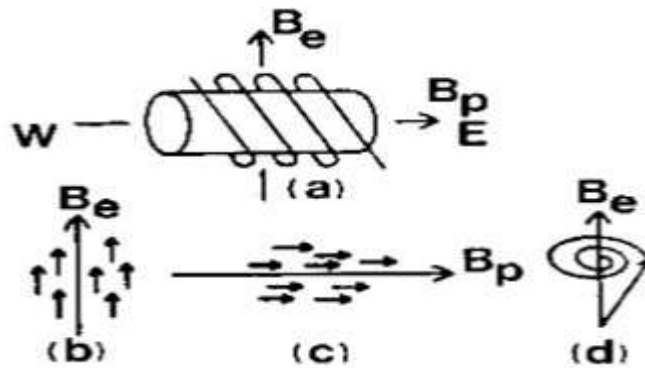


Figure 2.6: Principle of proton-precession magnetometer (a) Sensor with earth's magnetic field B_e and magnetic field of the instrument coil B_p (b) Alignment of protons in earth's field, (c) Alignment of protons due to applied field, (d) Precession of protons around earth's field after coil current is switched off. Adapted from (Philip *et al.*, 2011)

2.3.1 Theoretical framework for geoelectrical prospecting methods

This is an active geophysical method whereby the detection of surface effect produced by electric current flow in the ground is known as electrical prospecting method. It constitutes variable techniques unlike other geophysical methods (passive). Amongst are; self-potential, induced polarization, spectral induced polarization and electrical resistivity method. Using the electrical method, one may measure the potential, current and electromagnetic field that may occur naturally or introduced (Telford *et al.*, 1990).

The electrical method is used to study the horizontal or vertical discontinuity of rock electrical properties in one, two or three dimensional bodies of anomalous electrical conductivity (Philip *et al.*, 2011). There are three basic ways through which electric current

can be conducted through rocks and these are; the relative slow movement of ions within an electrolytic system that basically depends on the type of ions, ionic concentration and ease of mobility is termed electrolytic conduction, while the rapid ease of flow which allows electron to move freely, example as in metals is termed electronic conduction (ohmic) and the weakly conducting materials even at the introduction of external alternating current is been applied is termed dielectric conduction. Resistivity of a material is defined as the resistance in ohms between its opposite faces of a unit cube of the material. The SI unit of resistivity is the ohm-metre (ohm-m) and its reciprocal is termed conductivity (units is siemens (S) per metre; $1 \text{ Sm}^{-1}=1\text{ohm}^{-1}\text{m}^{-1}$). Figure 2.7 shows resistivity of rocks and minerals. Minerals such as native metals and graphite are good conductors while most rock forming minerals are not. However electrical current is carried in rocks through the pore water via the passage of ions. Hence, porosity is the major control of rock resistivity and by implication increases as porosity decreases. The uses empirical formula to express the effective resistivity in terms of resistivity and volume of pore water present in a rock was achieved by Archie.

Given by:

$$\rho = a\phi^{-b}f^{-c}\rho_w \quad 2.21$$

Where ϕ is the porosity, f the fraction of pores containing water of resistivity ρ_w and a , b and c are empirical constant. Resistivity of water can vary considerably according to the quantities and conductivities of dissolved materials.

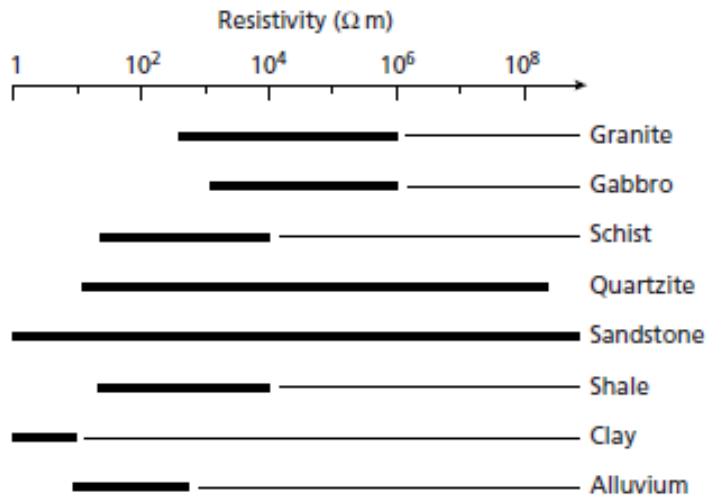


Figure 2.7: The approximate range of resistivity values of common rocks, adapted after Philip *et al.*, 2002.

The electrical methods have been improved in solving geologic issues right from 1920s to date. 1-D sounding surveys (1920s to 1980s) carry out measurements with different spacing between electrodes but with a common center. Data is usually plotted on log log graph as sounding curve. It assumes a simplified mathematical model for the subsurface that consist of horizontal layers. This informed layers correlates model properties with known geology.

The interpretation of data from one dimension sounding surveys can be automatically done using an inversion program. The apparent resistivity values and electrode spacing are entered together with the numbers of layers and estimated depth or thickness. The program then automatically adjusts the depth or thickness and resistivity of the layers until the calculated apparent resistivity values are close to the measured values. This gives a one-dimension picture of the subsurface, which is probably too simple in many cases.

The limitations of 1-D models are probably too inaccurate for most areas where there are significant lateral and vertical variations. However, this method is still used for extremely

deep aquifers and in many parts of the world where access to multi-electrode resistivity meter systems is limited.

The 1990s saw a rapid growth in two dimension surveys driven by availability of multi-electrode instruments, fast computer and automatic inversion software. A computer control program automatically selects the appropriate four electrodes for each measurement to give the lateral and vertical section (2-D coverage) of the subsurface. Through this time, it has become an important tool in hydrogeology, environmental, engineering and mineral sectors. It has enabled the mapping of complex structures previously not possible with one-dimension survey.

2.3.3 Basic concept of electrical resistivity method

Resistivity (ρ) which is an inherent physical property of a substance is its ability to resist the stream of current by a unit cube of that substance when voltage is applied across the opposite faces. The subsurface flow of current in resistivity survey is governed by a fundamental physical law known as the ohm's law. It is also expressed as a vector form for current flow in a continuous medium and is given as

$$J = \sigma E \quad 2.22$$

For an electric circuit, ohm's law gives

$$R = \frac{V}{I} \quad 2.23$$

$$\rho = \frac{VA}{IL}$$

Where, R is the resistance of current flow through the medium in ohms, V and I are the potential difference across a resistor and the current passing through it. A is area and L length.

This is represented in respect of electric field intensity **E**, current density **J** and conductivity **σ**

But

$$\rho = E/J \quad 2.24$$

$$E = -\nabla\phi \quad 2.25$$

Combining equation 2.23 and 2.24 we get,

$$J = -\nabla\phi\sigma \quad 2.26$$

According to Loke (2004), the current sources are in the form of point sources. In the case of an elemental volume ΔV surrounding the current source I located at (x_s, y_s, z_s) . The relationship between current density and current is given by;

$$\nabla \cdot J = \left[\frac{1}{\Delta V}\right]\delta(x - x_s)\delta(y - y_s)\delta(z - z_s) \quad 2.27$$

Equation 2.26 can be rewritten as

$$-\nabla \cdot [\sigma(x, y, z)\nabla\phi(x, y, z)] = \left(\frac{1}{\Delta V}\right)\delta(x - x_s)\delta(y - y_s)\delta(z - z_s) \quad 2.28$$

Where δ is the Dirac delta function hence equation 2.26 is the basic equation that gives the potential distribution in the ground due to point current source.

2.3.4 Potential for a homogeneous medium

In a homogeneous half space, the potential due to a single current electrode has a simple representation as

$$\phi = I\rho/2\pi a \quad 2.29$$

Where 'a' is the distance between the current and potential electrodes, ϕ is the potential due to a current source I and ρ is the resistivity of the medium

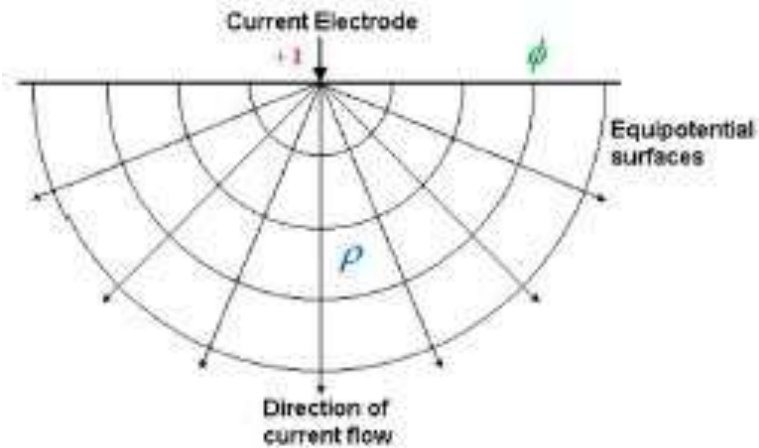


Figure 2.8: Current flow from a single surface electrode (Loke, 2004)

2.3.5 Electrical potential due to point current source

All resistivity survey in practice uses at most two current electrodes that consist of a positive and negative source. Figure 2.9 shows the potential values of a symmetrical pattern about the vertical plane at the mid-point between the two electrodes and the potential difference between the two electrodes is measured. From the current (I) and potential difference $\Delta\phi$ measurements, an apparent resistivity value is calculated. The apparent resistivity value ρ_a is calculate as

$$\rho_a = k \frac{\Delta\phi}{I} = KR \tag{2.30}$$

The calculated resistivity value is not the true resistivity of the subsurface but an apparent value that would give the resistivity of a homogeneous ground that will give the same resistance value for the same electrode arrangement.

\mathbf{K} is the geometric factor; \mathbf{R} is the resistance. The geometric factor \mathbf{K} is highly dependent on the arrangement of the four electrodes, where

$$\mathbf{K} = \frac{2\pi}{\left(\frac{1}{r_{c1p1}} - \frac{1}{r_{c2p1}} - \frac{1}{r_{c1p2}} + \frac{1}{r_{c2p2}}\right)} \tag{2.31}$$

2.3.6 Electrical field survey measurements

In an electrical field survey, the resistivity of the subsurface is measured by passing artificial current through the ground with the aid of metal or graphite electrodes. Four electrodes are planted into the ground (Figure 2.10). An electric current of 10mA to 3A is injected into the ground using electrodes C_1 and C_2 . The resulting potential difference at two points on the ground surface is measured using two electrodes, P_1 and P_2 . Changes in the ground resistivity will cause deviation in the current flow and the resulting voltage difference.

2.3.7 Electrical properties of metallic and mineral ores

Figure 2.11 shows how most metallic sulfides such as pyrrhotite, galena and pyrite have typically low resistivity values of less than $1\Omega.m$. The resistivity value of a particular ore body can differ greatly from the resistivity of the individual crystal. Factors such as the nature of the ore body (massive or disseminated) have significant effect.

Graphitic slate has a low resistivity value, similar to the metallic sulfides, which can give rise to problems in mineral surveys. Most oxides, such as hematite, do not have a significantly low resistivity value exception of magnetite.

Iron has extremely low resistivity values. Chemicals that are strong electrolytes such as potassium chloride and sodium chloride can greatly reduce the resistivity of ground water to less than $1\Omega.m$ even at fairly low concentrations. The effect of weak electrolytes such as acetic acid is comparatively smaller.

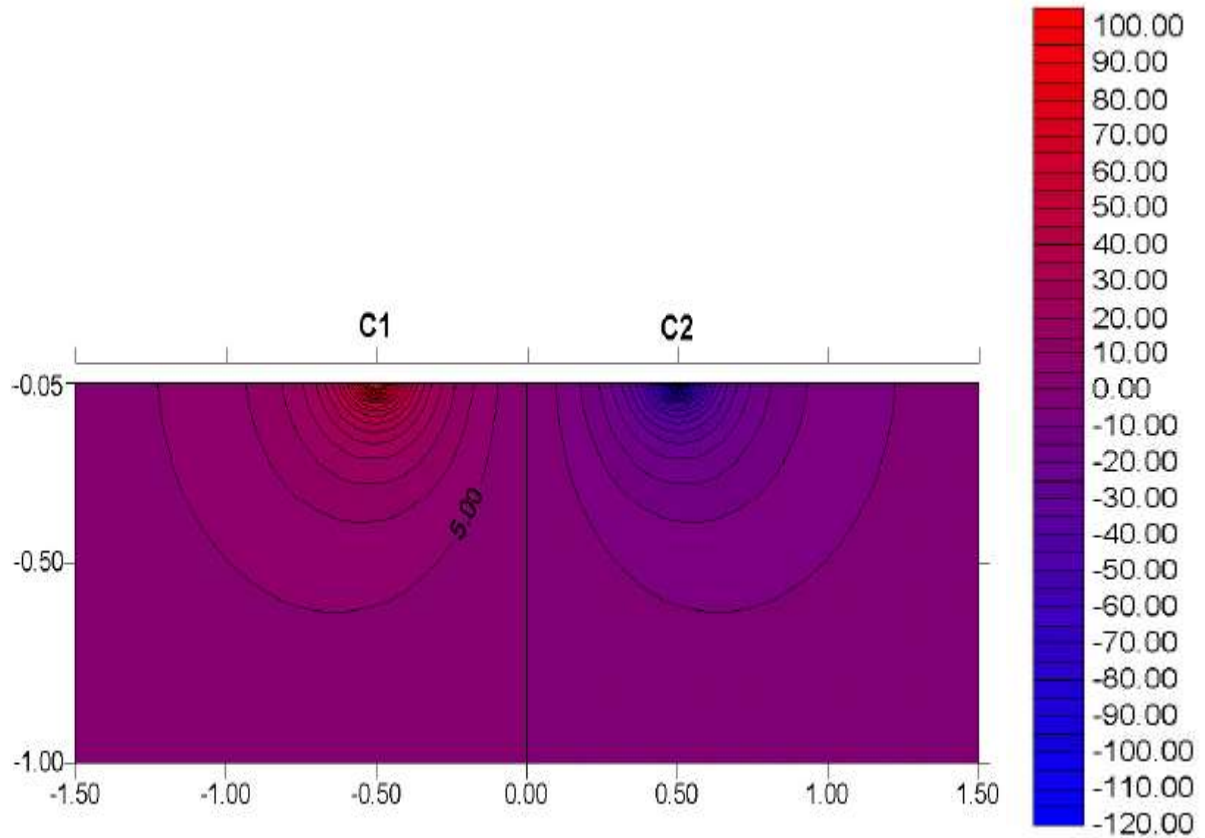


Figure 2.9: The potential distribution caused by a pair of current electrodes 1 meter apart with a current of 1 ampere and a homogeneous half-space with resistivity of 1 Ω . m (Loke,2004).

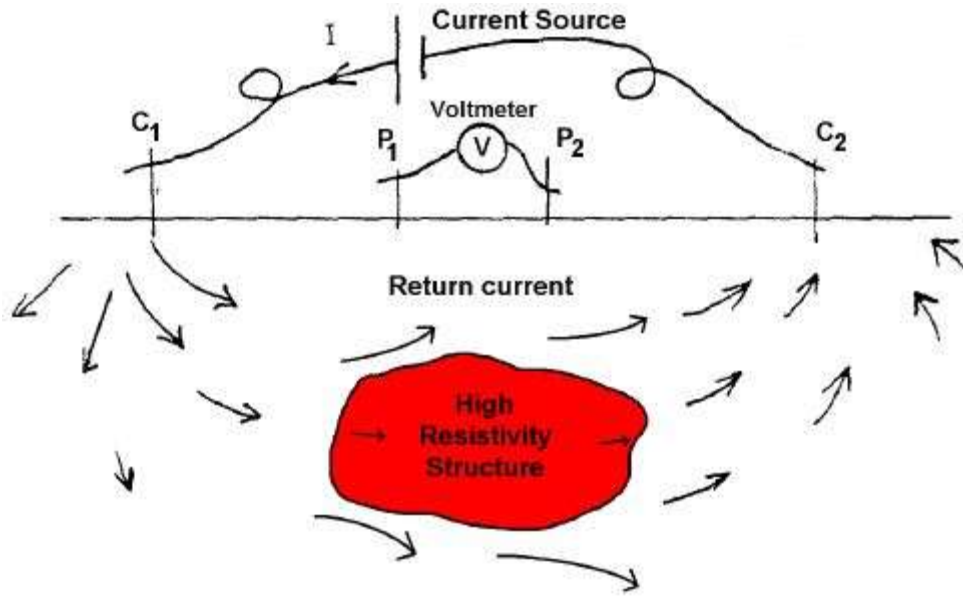


Figure 2.10: Basic setup for a resistivity survey.

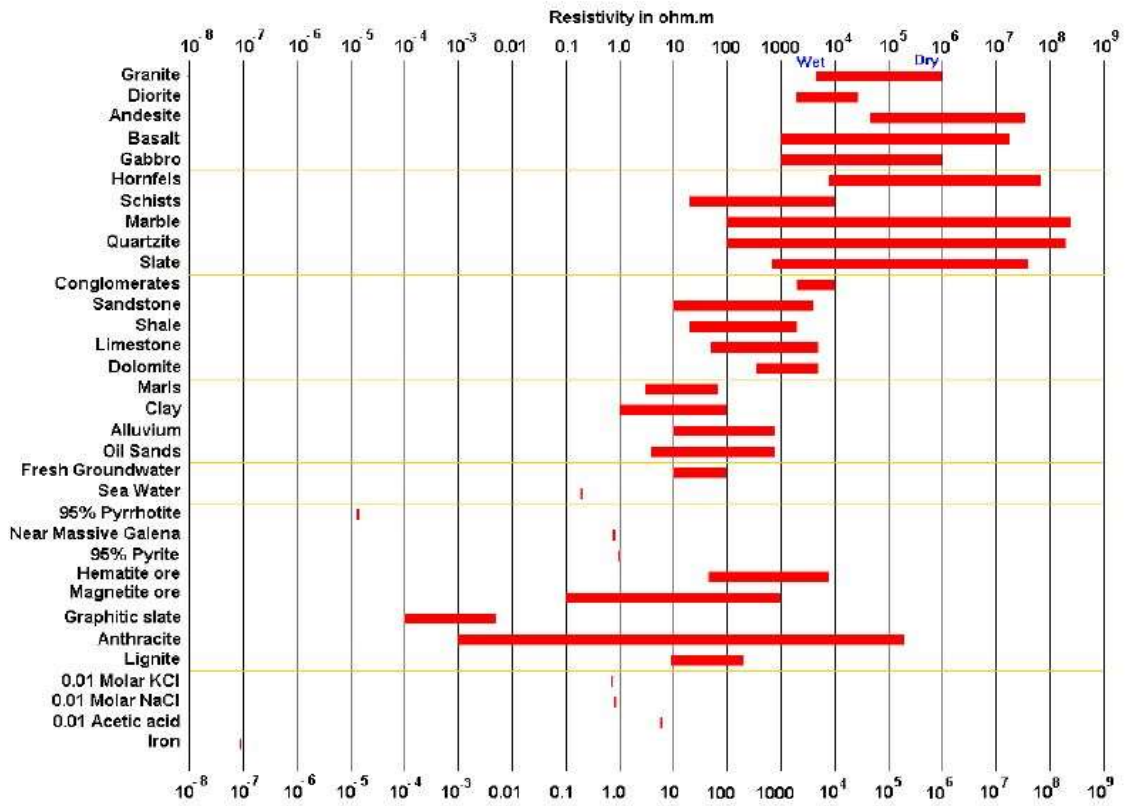


Figure 2.11: The resistivity of rocks, soil and minerals (Adapted from Loke, 2004)

2.3.8 2-D Electrical imaging surveys (ERT)

The 2-D electrical resistivity tomography survey is usually carried out with a computer controlled resistivity meter system connected to a multi-electrode cable system. The control software automatically selects the appropriate four electrodes for each measurement to give 2-D coverage of the subsurface. A large variety of arrays and survey arrangement can be used with such a system. To obtain a good 2-D picture of the subsurface, the coverage of the measurement must be carried out in 2-D as well (horizontal and vertical).

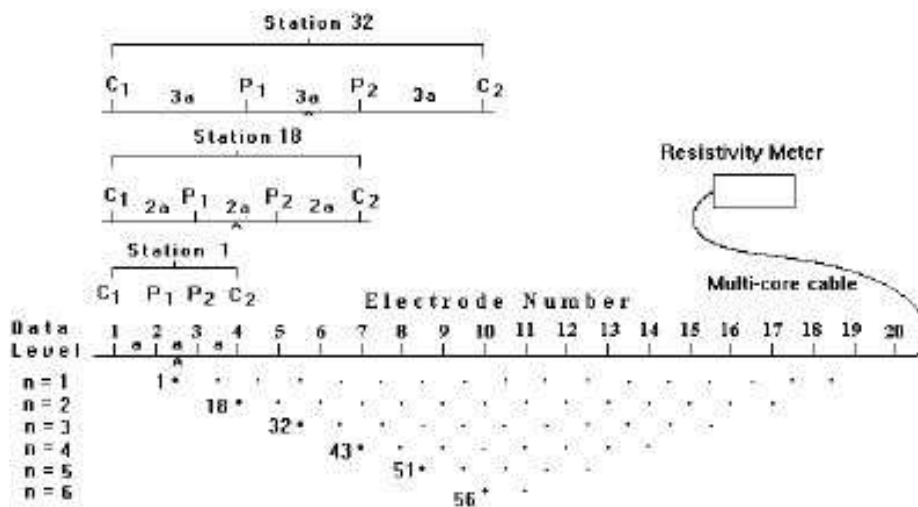


Figure 2.12: Sequence of measurements to build up a pseudosection

Figure 2.12 shows a sequence of measurements for the Wenner alpha electrode array for a system with 20 electrodes where all the possible spacing from $1a$ to $6a$ are measured across the line. After the field survey the resistance measurements are usually changed to apparent resistivity values. The purpose of the inversion is to convert the apparent resistivity values into a model section. The conversion is carried out on a computer system using an automatic inversion program. The inversion process applied Res2Dinv code by which forward modeling subroutine will be used to calculate the apparent resistivity values, the standard

least-squares optimization technique will be used for the inversion routine. Using the following equation;

$$[J_i^T J_i + \lambda_i W^T W] \Delta q_i = J_i^T g_i - \lambda_i W^T W q_{i-1} \quad 2.32$$

Where \mathbf{W} is the roughness filter, λ is roughness filter damping factor, \mathbf{q}_{i-1} is the current inversion model, Δq_i is the change in model resistivity to be calculated, \mathbf{g} is the data misfit, difference between measured and calculated apparent resistivity values and \mathbf{J} is the Jacobian matrix of partial derivatives or sensitivity.

The routine used constraints to minimize the square of the difference between the observed and the calculated apparent resistivity values, the effect of the side block was reduced, so that the calculated value not unreliably exaggerated. Since there are very large resistivity variations near the ground surface, a model of width half the unit spacing was used to give the optimum inversion results. The standard least-squares optimization technique converged after 5 to 10 iterations with a RMS misfit between 10% and 40%.

CHAPTER THREE

3.0 MATERIALS AND METHODS

3.1 Materials

Materials employed in the entire exercise are:

- i. Resistivity meter (McoHms 2115 OYO) and Accessories
- ii. Magnetometer (Geometrics G856AX)
- iii. Handheld Global Positioning System (GPS) device: Garmin (etrex 10) and GPSMAP 78sc
- iv. Compass-clinometer, geological hammer, hand lens.
- v. Tape, ribbon and marine rope.
- vi. Topographic map of Minna sheet 164 SW.
- vii. Data processing software to be used include; Oasis montage, RES2Dinversion and Rockwork.

3.2 The Research Method

3.2.1 Field geological mapping

Preliminary reconnaissance survey was carried out to demarcate the research study area using the Global Positioning System (GPS). This involves altitude reading, observation of landscape, outcrop location recording and drainage pattern observation. Geological mapping was carried out to have a detailed spatial distribution of outcrop and associated structures (joints and faults) orientation were measured.

The geologic field mapping was achieved through the following processes

- Preliminary reconnaissance and traverse lining with pegs

- Inter line spacing of 50m and inter sample spacing of 10m using GPS on ground measurements.
- Geologic field work

Geologic field works were undertaken in the study area to relate the effect of the structures in field to result obtained from the interpretation of the magnetic data. Structural features (fault and joint) orientations were ascertained to establish principal structural trends that strongly agree with the regional trend. Identification of rock sample was achieved using hand specimen of the mafic mineral index.

3.2.2 Acquisition of total magnetic field data by ground magnetic

Ground magnetic survey equipment (Plate III) deployed for the exercise is the Geometric 857AX Proton Precession Magnetometer with external GPSMAP 78sc Garmin. The standard system is used as a mobile instrument for total magnetic intensity sequentially at discrete locations. Appropriate accessories were setup and configured for measurement of the differential magnetic field over the survey area which records the temporal changes in the magnetic intensity at a fixed selected location (point) to acquire base station readings. Eleven traverses were established perpendicular to the strike of rocks in the area. Fifty-one (51) stations were conducted along the traverses. Fifty meter (50) m inter profile spacing and ten meter (10) were deployed.

Base station method for correction of diurnal variations is used while the area selected for base station was magnetically clean, that is free from moving automobiles and is not close or on top of any major outcrop neither under power line. The stored data from the instrument was downloaded on a computer system. The downloaded data is later saved in an Excel Spread-sheet for easy accessibility. All Magnetics Stations were tied to their respective

coordinates. Quality Control and Quality Assurance was strictly applied on the raw data through visual inspection. This is useful in making sure that all survey specifications are been adhered to. Observed geology, cultural features and all possible source of noise shall aid in the execution of Quality Control and Quality Assurance on the data.



Plate 111: Geometrics 857 AX proton precession Magnetometer

3.2.3 Magnetic data filtering

It is germane to filter magnetic data before interpretation and this involves wide range of transformation and mathematical simulations of data. The aim is to simplify anomaly features by relating them to observed rock properties. The filtering tools includes; euler deconvolution and analytical signal. The adaptation of data filtering process bears significance with relation to regions under investigation for improved qualitative and quantitative interpretation.

3.2.4 Interpretation of magnetic anomalies

Interpreting magnetic data collected near the earth's magnetic equator is more difficult than high latitude magnetic data due to the intensity around the equator which is smaller and the ambient inducing field is horizontal (Les *et al.* 2000). The complexities associated in the interpretation of magnetic data uniquely differentiate it from other potential field method. A good characteristic of the magnetic anomaly of a finite body invariably contains positive and negative elements arising from the dipolar nature of magnetism. Thus intensity of magnetization is a vector hence the magnetization in a body closely controls the shape of anomalies. The intensity of magnetization largely depends on the amount, size, shape and the distribution of ferromagnetic materials (Philip *et al.*, 2002)

The qualitative interpretation takes relevance of nature of wavelength and amplitude as it relates to magnetic causative bodies with due cognizance of regions of implication. For instance, short-wavelength, high-amplitude with negative to the north and positive to the south with an elongation in the east-west direction in the mid-latitude of the northern hemisphere suggest a near surface, moderate to high magnetic susceptible features. In carrying out a quantitative interpretation of magnetic anomalies, the salient direct methods is best suit with several mathematical equations exist for total field anomalies (Philip *et al.*, 2002). It attempts to give a realistic shape, size direction and depth to magnetic bodies. A more complex, but more rigorous method of determining the depth to magnetic sources derives from a technique known as *Euler deconvolution* (Philip *et al.* 2002). Euler's homogeneity relation can be written:

$$(x - x_o) \frac{dT}{dx} + (y - y_o) \frac{dT}{dy} + (z - z_o) \frac{dT}{dz} = N(B - T) \quad 3.1$$

Where (x_0, y_0, z_0) is the location of a magnetic source, whose total field magnetic anomaly at the point (x, y, z) is T and B is the regional field. N is a measure of the rate of change of a field with distance and assumes different values for different types of magnetic source.

The analytical signal filter of the potential field determines the shape, size and exact location of magnetic causative bodies.

Given as:

$$A(x, y, z) = \left[\frac{\delta m}{\delta x} \right] x + \left[\frac{\delta m}{\delta y} \right] y + \left[\frac{\delta m}{\delta z} \right] z \quad 3.2$$

where M is the magnetic field

3.3.1 Acquisition of geoelectrical data

Electrical resistivity equipment employed for the exercise is the improvised resistivity meter calibrated with McOhm 2115 OYO meter (Plate IV). The measurement was conducted along the East-West direction, measuring 200m. The reading was taken on all measurement points generating 253 data points. Anomalously high value of apparent resistivity is often associated with quartz and banded iron formation (BIF).

Resistivity data was basically acquired with respect to high and low magnetic intensity which constitutes signature characteristic of potential mineralization. The Wenner Alpha array was adopted in the entire exercise. A profile of 200m that runs in the East-West direction was measured to detect conductivity of mineralization, figure 4.6. RES2DINV software was used for the 2D-inversion of the resistivity data.

Quality control enhancing parameters were strictly adhering to for quality data acquisition. These control parameters include; good connection within cables to prevent leakage. Cables are appropriately label for quick identification. Electrodes are driven down to have proper contact with the soil and making sure data points are appropriately taken.

Acquired data are uploaded on the computer using notepad. These data are processed using Res2D inversion software before interpretation.



Plate IV: Geoelectric data acquisition

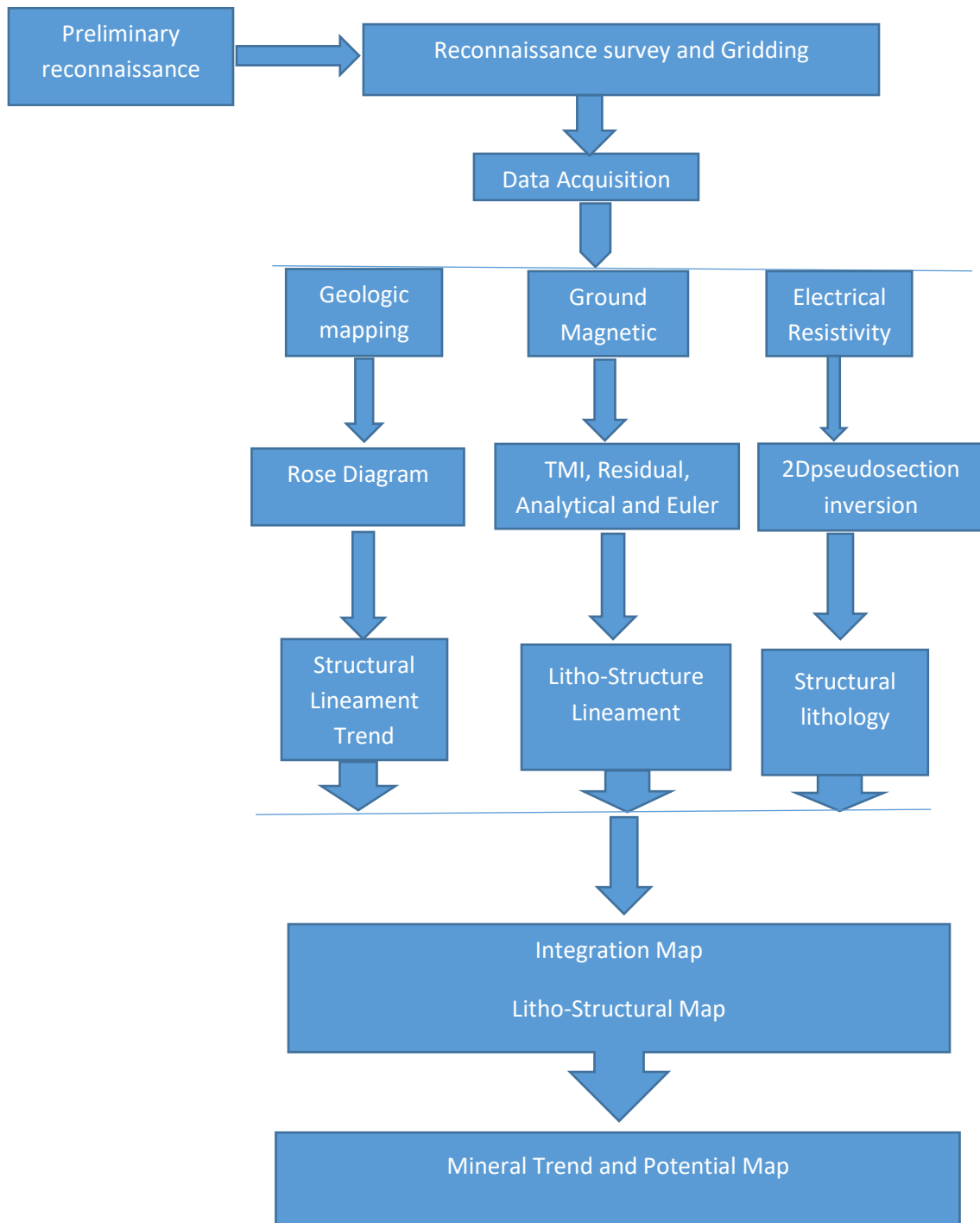


Figure 3.13: Flow chart showing the method of study

CHAPTER FOUR

4.0 RESULTS AND DISCUSSION

4.1 Results of Field Geology Mapping

The result of the geology mapping is presented on Figure 4.1 which expresses the observed rock type within the study area.

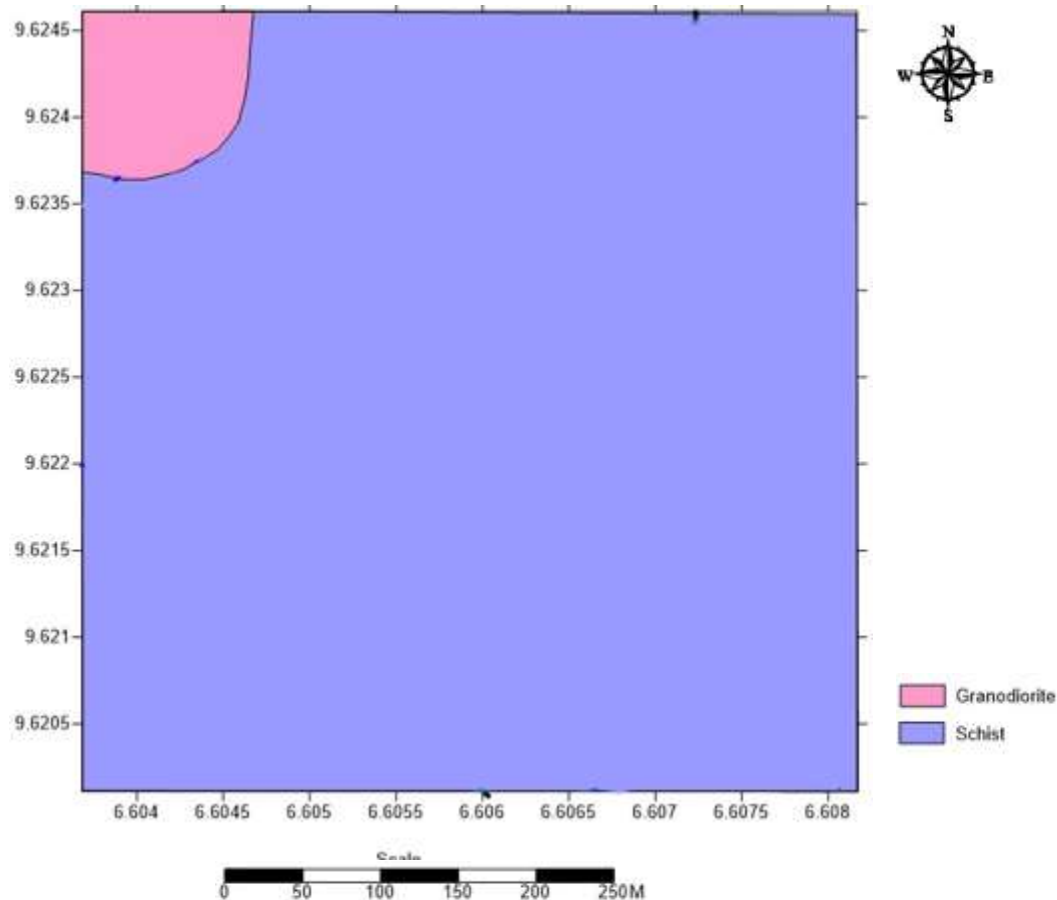


Figure 4.1: Geologic Map of the Study Area

Figure 4.1 shows the mapped area basically constitutes two major rock units using the mafic mineral index. These includes; Schist and Granodiorite. The former is the dominant rock intruded by the later. The granodiorite is exposed within the stream channels around the North western part of the study area. These rocks have undergone some sorts of deformation

and shearing which gives resultant structural features that could host potential mineralisation.

Plate V and VI reveals structures such as fault, fracture (veins) and joint that is possibly mineralised.



Plate V: Quartz vein (filling of openings, cracks or fracture in rocks with quartz)



Plate VI: Set of joints/fractures

The direction of the structure measured establishes trends of principal and minor mineralised zones with relation to the regional trends. The principal trends of structures are in the NNE-SSW, NE-SW and minor trends are N-S and E-W direction (Figure 4.2)

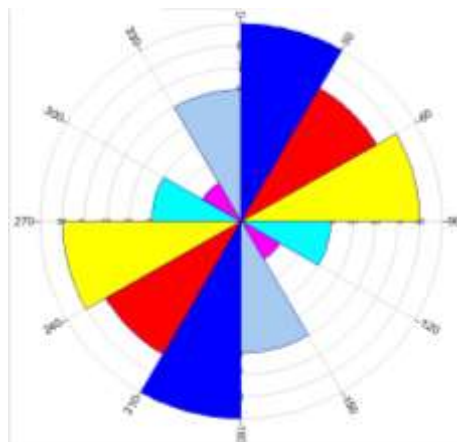


Figure 4.2: Rose diagram showing trends of structural features (joint /fracture)

4.2 Results of Total Magnetic Intensity Measurement

The total magnetic intensity (TMI) data are presented in a map form in figure 4.4. Figure 4.5 shows the contour map of total magnetic intensity raw data. It clearly exhibits the trend of structure which gives evident anomaly features in relation to the close packed of it. The residual anomaly minima and maxima amplitude signature shows positive magnetic amplitude (maxima) ranging from -99 nT to 82 nT (Figure 4.6) which is a characteristic features of mapped rock within the study area. This wide contrast in values suggests subsurface presence of ores, such as gold associated with rocks of high magnetic susceptibility. The residual magnetic field intensity map, generally show majorly NE-SW and E-W trending anomalies with few trending in N-S (Figures 4.6) which is evidently witness on rose diagram (Figure 4.2) and lineament map (Figure 4.3). Haruna (2017) reported that the stress pattern of the Nigerian landmass changed appreciably from N-S and NNE-SSW trend to NE-SW and ENE-WSW trend from Pan African to Early Cenozoic. Thus the NE-SW and ENE-WSW represent the imprints of Pan African tectonism on the study area. This shape of magnetic signature obtained in the ground magnetic survey generally suggests a step or an edge structures like dyke or intrusion, such structures are of interest may hold mineralization at certain depth.

The red arrow on the South Eastern part of residual map depict tunnel section of the artisanal mining. This excavated portion is suggestive of mere intuition which in most cases miss lineament structure as seen from the lineament map. On the profile line the lineament is intercepted at 120 m East-West direction. Corroboratively, orogenic activities and hydrothermal alteration is observed on fragment of ferruginous quartz vein with flakes of gold and other associated minerals. Also, it is revealed that areas signifying high magnetic susceptibility with corresponding low resistivity are quite suggestive of eluvial deposit. The

broad black coloured line is the resistivity profile line, the red no fill arrow marks the starting point, it runs in the East-West direction. Figure 4.7 shows the spatial distribution of depth to magnetic source body with the deepest source at 25m while the shallowest is 8m. Thus edge detection of magnetic body was controlled by Analytical signal which invariable inform the choice location for electrical resistivity (Figure 4.8).

The magnetic data were plotted into color coded contour maps. The high magnetic portion are within the range of pink to red zones of the total magnetic intensity while the blue to green zone are low magnetic intensity. This is directly interpreted qualitatively. Four indicative exploration guides were used to characterised potential zones for mineral prospecting. Figure 4.4 shows the general trend of magnetic intensity, indicative of the high and low intensities. A more detailed anomalous grid is observed on Figure 4.6 of the residual magnetic map. It gives a qualitative interpretation of features present. The resultant effect is as a result of the magnetic source bodies at varied depth as seen from Figure 4.7 and edges of the magnetic bodies on Figure 4.8.

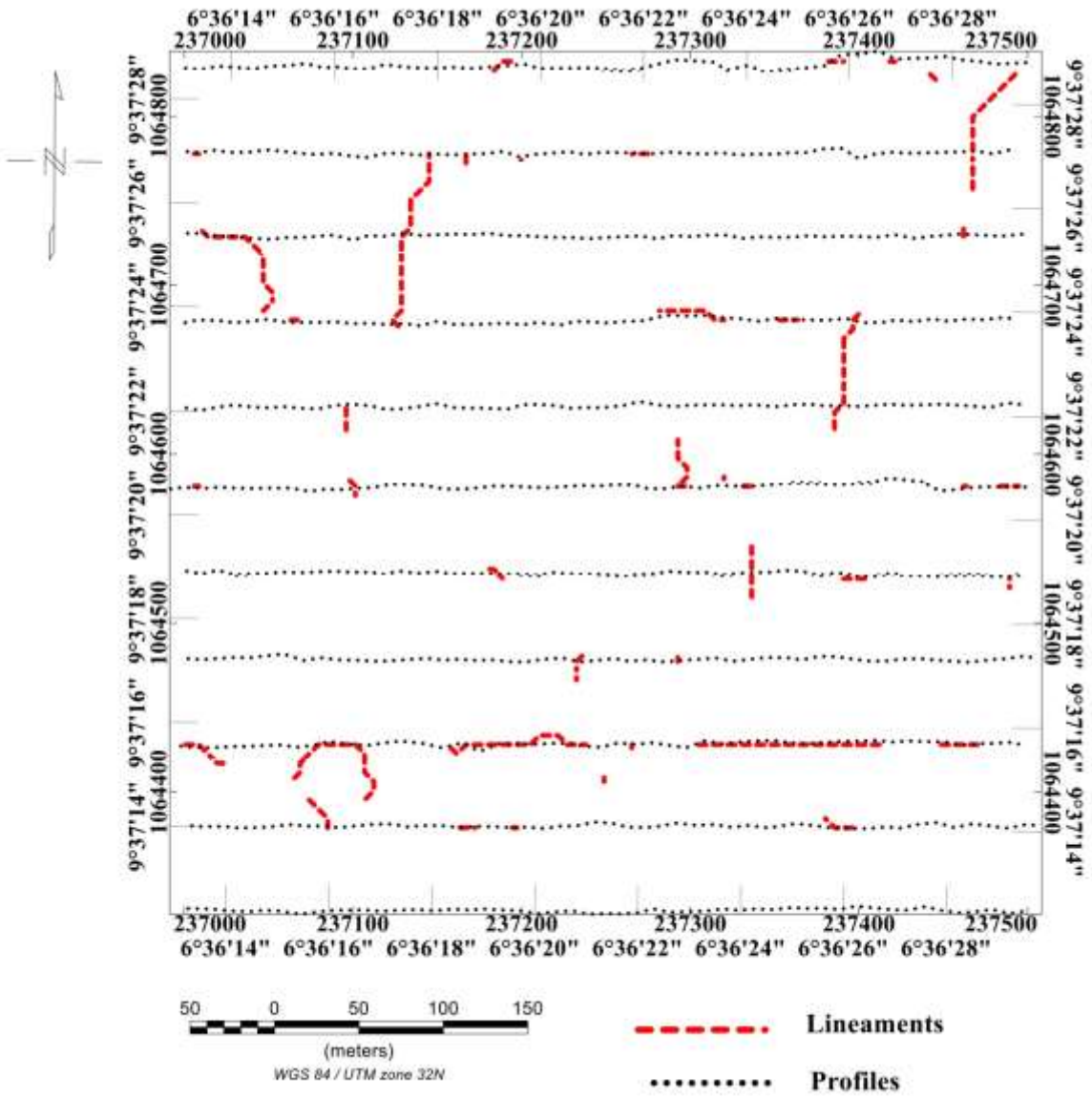


Figure 4.3: Lineament map produced from the analytic signal map of the study area.

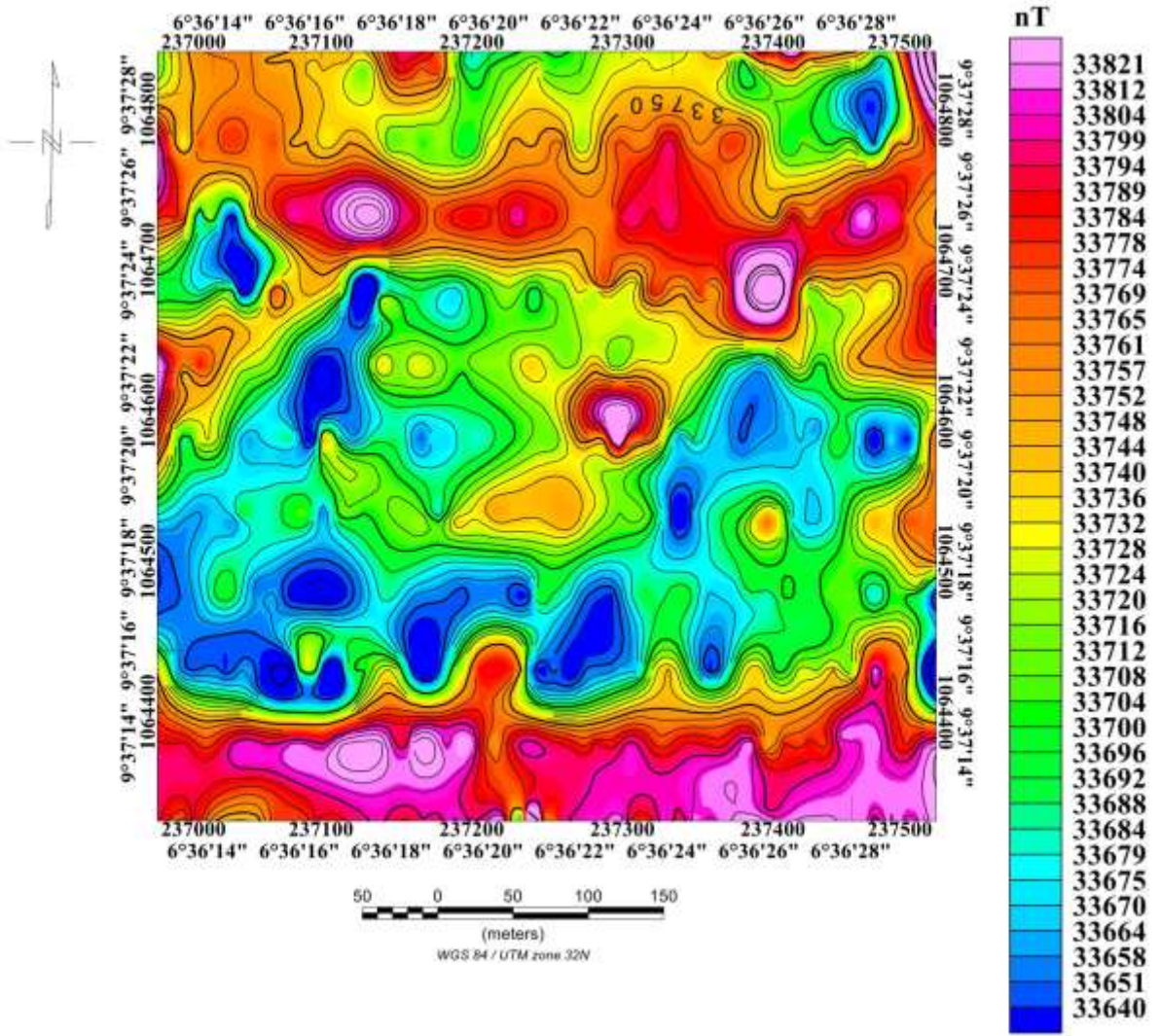


Figure 4.4: Total Magnetic Intensity Map of the Study Area

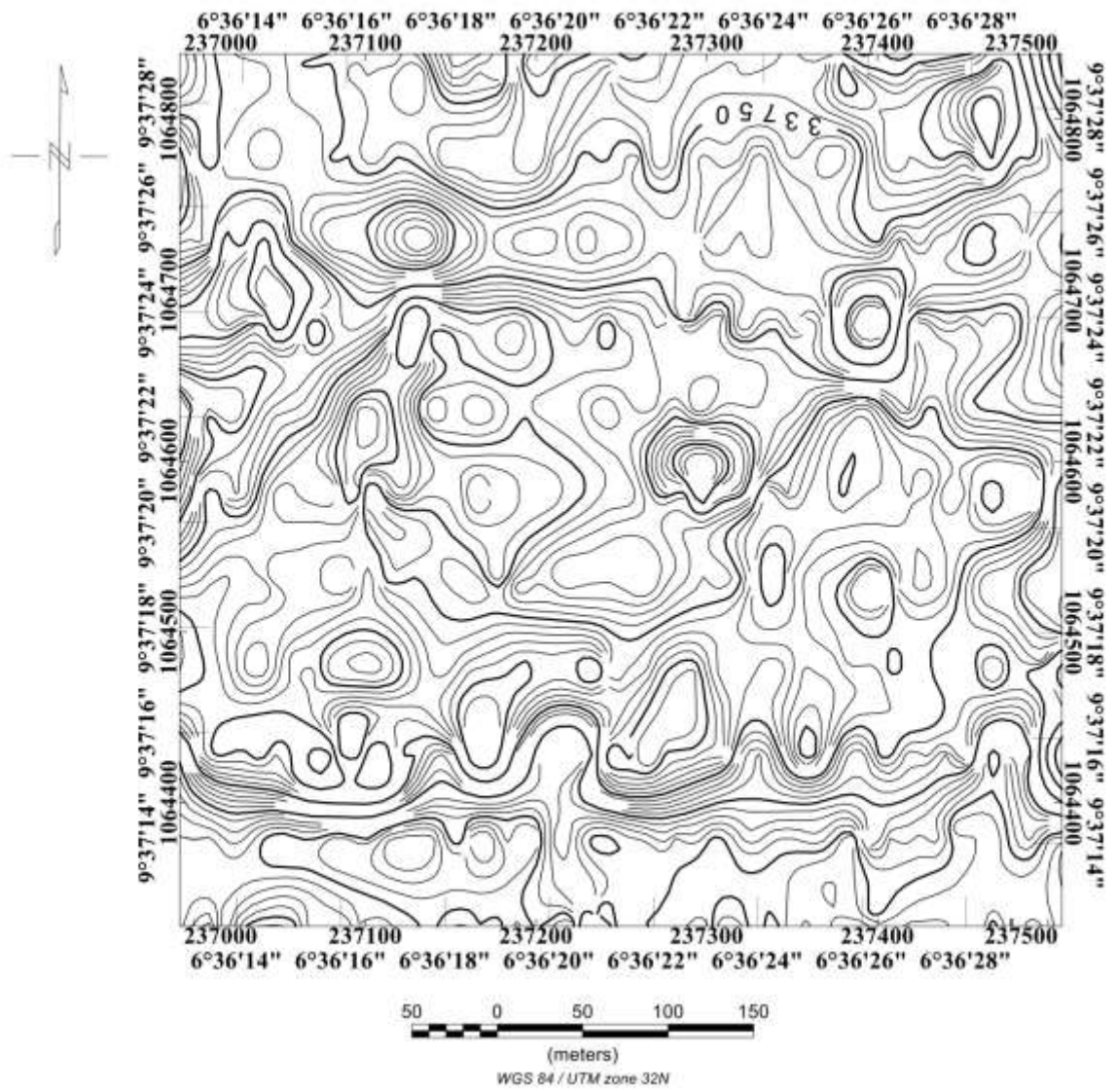
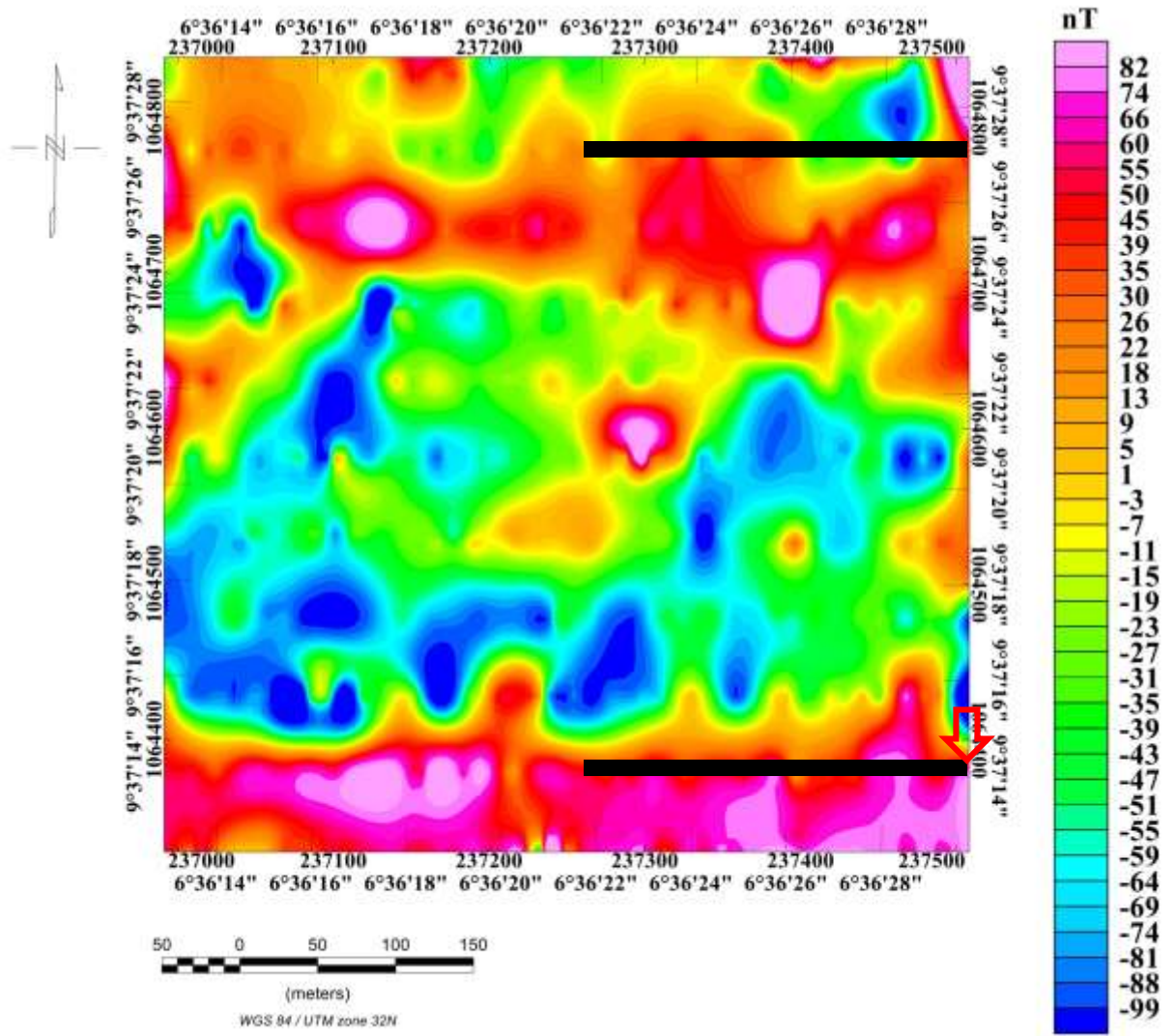


Figure 4.5: Total Magnetic Intensity Contour Map of the Study Area.





-  ERT Profile
-  Trench

Figure 4.6: Residual Map of the Study Area

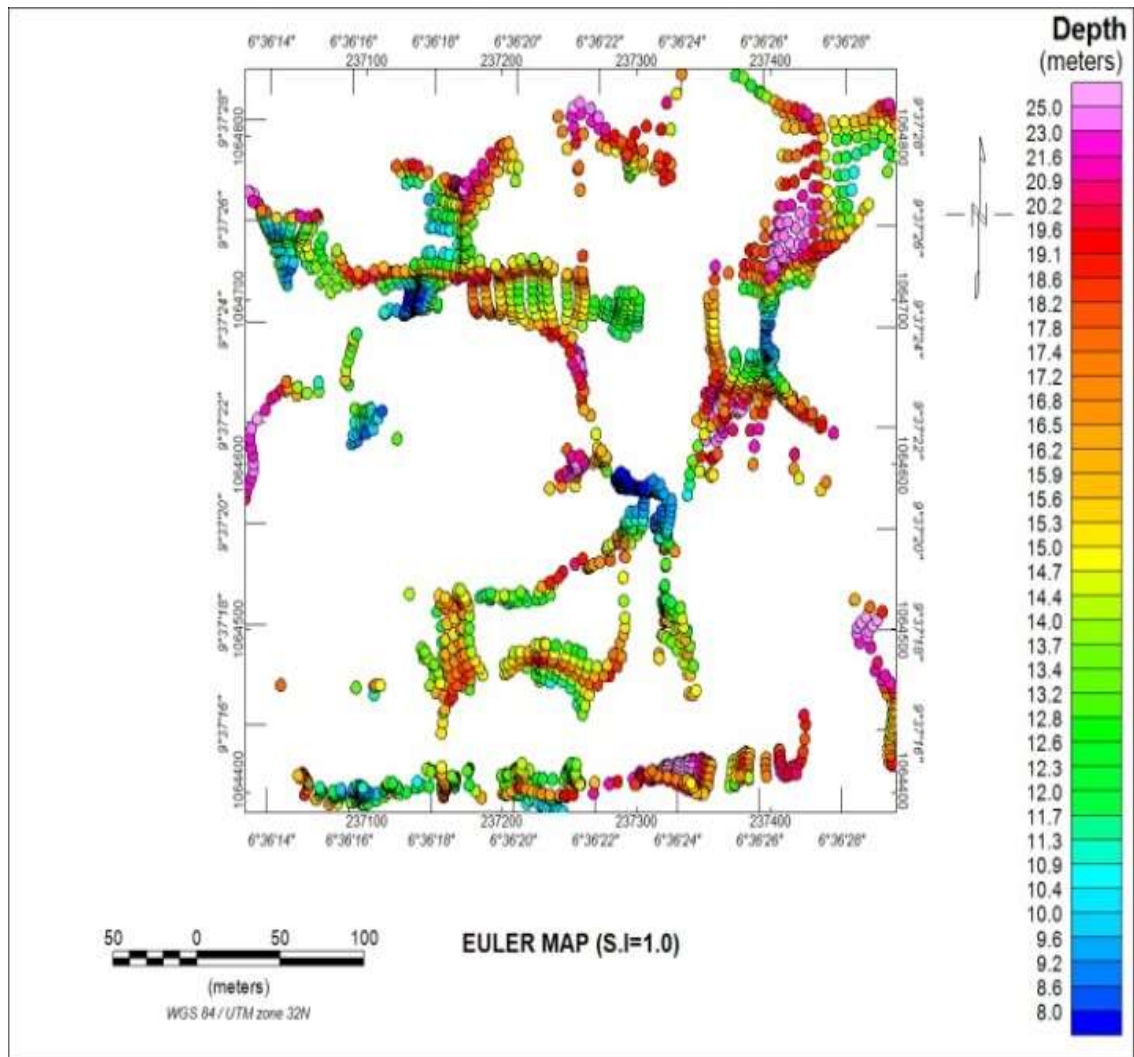


Figure 4.7: Euler map of study area showing depth to source body

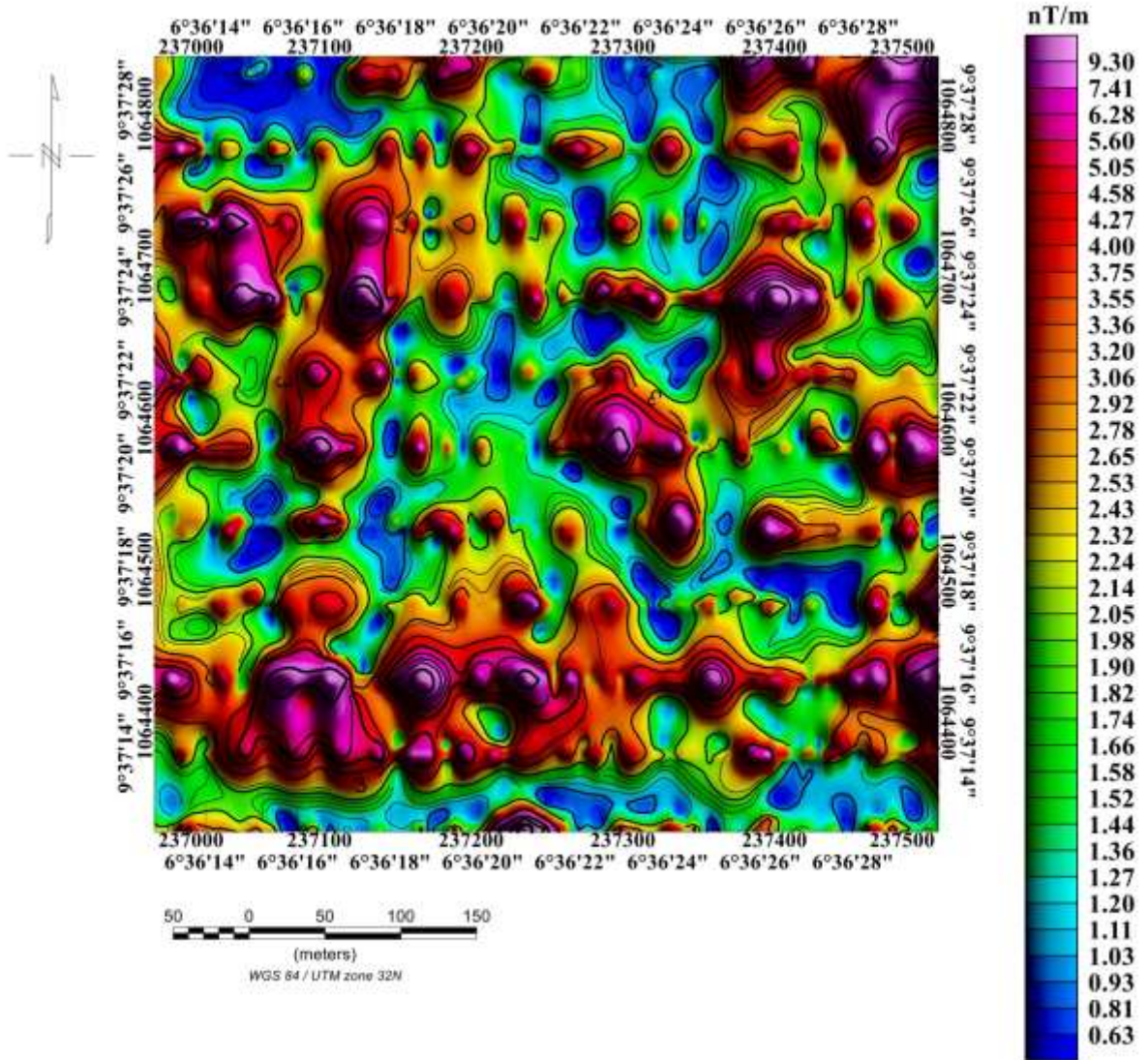


Figure 4.8: Analytic Signal Map with Contour of the Study Area.

4.3 Result of Geoelectrical Resistivity Measurement

Primary gold occurrences in the northern Nigeria schist belts are associated with sulphide mineralization, hence low resistivity. Quartz veins are characterized by high resistivity (low conductivity). Most primary gold mineralization in the schist belts commonly occurs in quartz veins within different lithologies, therefore geophysical characteristics of the quartz veins is another important factor in mineral prospecting and delineation of gold deposit (Samson *et al.* 2014)

The color coded sections of the geoelectrical resistivity measurement is indicative of high resistivity and low resistivity which ranges from pink to red and blue to light green. Two points designated as magnetic high and low; South-East and North-East of the residual magnetic were chosen as sites for apparent resistivity pseudo-section. 2-D inverted resistivity shows a qualitative idea of resistivity distribution in the subsurface.

Figure 4.9 shows the result of 2-D profile section from the residual magnetic map. Along this profile line there is no evident activity of artisanal mining. Rubbles quartz scattered on the surface. This selected portion specifically has high magnetic intensity which necessitated resistivity probing. At 80m point on the profile line lies lineament feature as shown on the lineament map. Corroborating this feature with the pink dyke like structure observed on the 2-D pseudo-section suggest a mineralised quartz vein. Also, portions beyond this point with high magnetic intensity and corresponding low resistivity are possible sites for eluvial deposits. Figure 4.10 shows 2-D resistivity tomography map with the starting point being the edge of the tunnelling by artisanal miners. Excavated materials showed quartz vein intruding the schist(host) rock. Prior to 120m, high magnetic susceptibility with low resistivity was observed, which is suggest the presence of eluvial deposits.

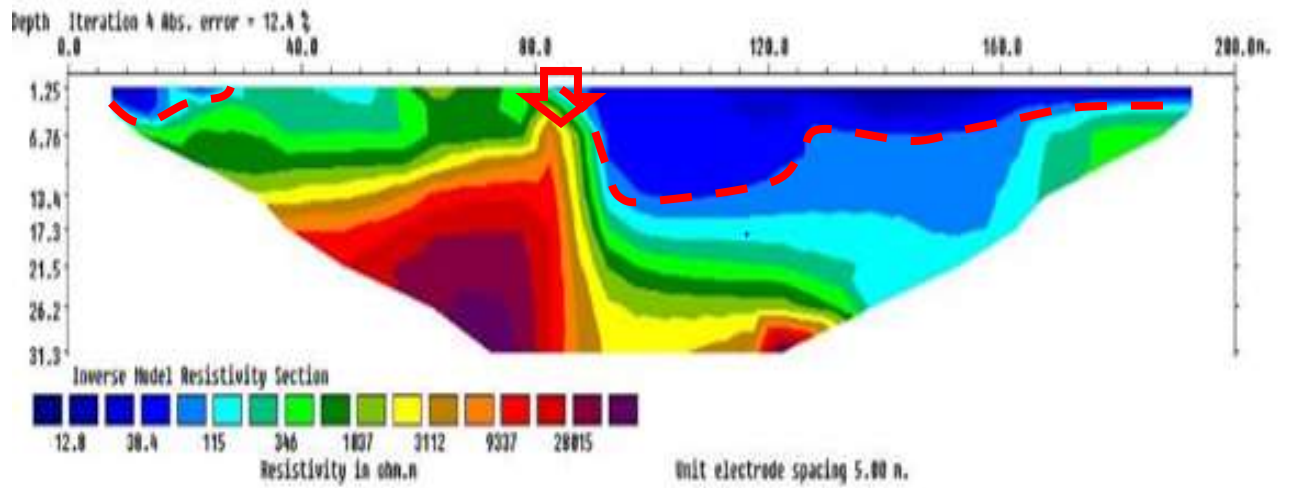


Figure 4.9: 2-D Resistivity Profile on 9° 37' 28.0''N and 6° 36' 28.0''E

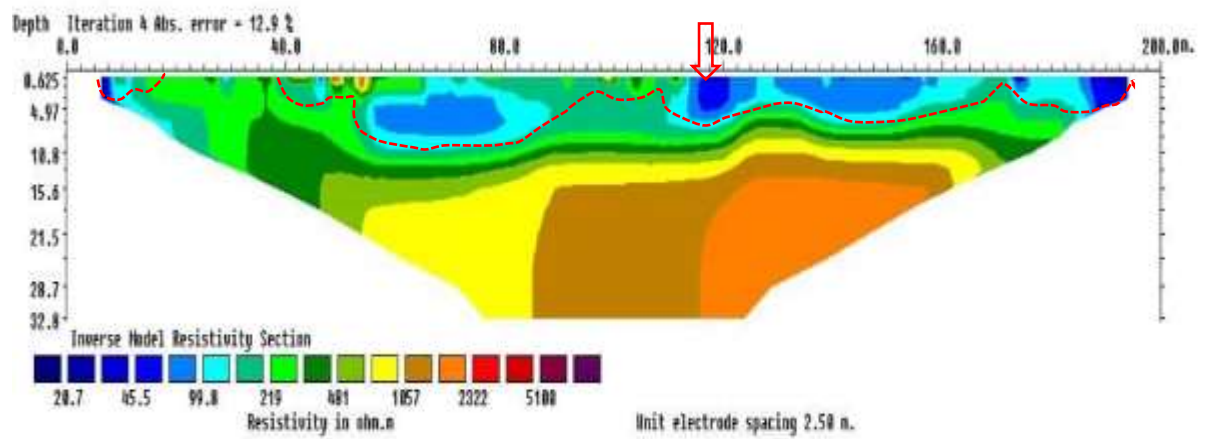


Figure 4.10: 2-D Resistivity profile on 9° 37' 16''N and 6° 36' 28.0''E

CHAPTER FIVE

5.0 CONCLUSION AND RECOMMENDATION

5.1 Conclusion

The study was able to establish the surface structure pattern, total magnetic anomaly pattern and electrical anomaly pattern indicate subsurface linear structure suspected to be quartz veins that do host gold deposits. This structure are potential zones for mineralization which is in accordance with the lineament map and edge detection of the magnetic bodies. The ground magnetic was used in delineating areas with high magnetic intensity in relation to low intensity. Also depth to magnetic source body is established. The zones of mineralization associated with lineament map as well as eluvial and placers deposits is in consonant with the lineament map that are of orogenic and hydrothermal zones of alterations.

Minerals are structurally controlled, delineating this structure requires adherent to geophysical and geologic techniques as established. Combining the results of geologic structures and geophysical methods reveal a wide range of linear structures suspected to be quartz veins which are believed to host ore mineralisation as identified. Responses to physical parameters also revealed that some of the structures delineated from the magnetic data are conductive while others are non-conductive, while some are within a resistive host and others are within a conductive host. Several of such trending mostly NE-SW, E-W and N-S were identified.

5.2 Recommendation

Based on the geological, magnetic and geo-electrical analysis, it is therefore recommended that geochemical sample analysis and drilling be carried out on designated points to fully ascertain grade of mineralisation.

5.3 Contribution to Knowledge

This study in its entirety was able to use ground magnetic and geoelectrical method as a geophysical survey technique for the prospecting of gold mineralisation. It establishes the trend of structure in the study area to be NE and SW been the principal joint direction. The magnetic effect of source bodies was established with the deeper source at 25 m and shallow source at 8 m. The eluvial deposits was also established at 5 m and 13.4 m respectively.

References

- Abdullahi, S. & Alabi, A.A. (2018, October). Geophysical evaluation of gold potential in Southwestern part of Kaffin Koro, Northwestern, Nigeria. *Journal of Applied Geology and Geophysics*, 6(5), 56-66.
- Abubakar, Y. I. (2012, MAY). An integrated technique in delineating structures: A case study of the Kushaka Schist Belt Northwestern Nigeria. *International Journal of Applied Science and Technology*, 2(5), 3-6.
- Adetona, A. A., Salako, K. A. and Rafiu, A. A. (2018, April). Delineating the lineaments within the major structures around Eastern part of lower Benue trough from 2009 Aeromagnetic data. 3(1), 175-179.
- Adree Octova & Dedi Yulhendra. (2016). Iron ore deposits model using geoelectrical resistivity method with dipole-dipole array. *MATEC*. Padang: State University of Padang, Indonesia. doi:10.1051/mateconf/201710104017
- Ajibade, A.C., Woake, M. and Rahaman, M.A. (1989). Proterozoic crustal development in the Pan-African Regime of Nigeria . In C. Kogbe, *Geology of Nigeria, 2nd edition* (pp. 57-69). Jos: Rock view (Nigeria) Limited.
- Alile, O. M., Aigbogun, C. O., Enoma, N., Abraham, E. M., and Ighodalo, J. E. (2017, June). 2D and 3D Electrical Resistivity Tomography (ERT) investigation of mineral deposits in Amahor, Edo State, Nigeria. *Nigeria Research Journal of Engineering and Environmental Sciences*, 2(1), 215-231.
- Andrew J., Alkali A., Salako K. A., Udensi E.E. (2018, may). Delineating mineralisation zones within the Keffi-Abuja Area Using Aeromagnetic Data. *journal of geography, environment and earth science*, 15(3), 1-12.
- Bernard Siachingoma and Renisia Tipedze. (2012). Using Induced Polarization as follow up to Magnetic method in prospecting for gold at Lady A claims. *International Journal of Science and Research*, 3(7), 152-156.
- Bruce W. D. Yardley & James S. Cleverley. (2013, October). The role of metamorphic fluids in the formation of ore deposits. *Geological Society of London*, 393, 117-134. doi:10.1144/sp393.5
- Ejebu, J. S., Unuevho, C. I. and Abdullahi, S. (2018). Integrated geosciences prospecting for gold mineralisation in Kwakuti, North-Central Nigeria. *Journal of geology and mining research*, 10(7), 81-94.
- Fareed, M. (2016). Application of Magnetic and Electrical Geophysical Methods in Delineating Auriferous Structures in the Sefwi Belt of Ghana.

- Haidarian Shahri, M. R., Karimpour, M. H. and Malekzadeh, A. (2010). The exploration of gold by magnetic method in Hired Area, South Khorasan, a case study. *Journal of the Earth and Space Physics*, 35(4), 33-44.
- Haruna, I. (2017, February). Review of the Basement Geology and Mineral Belts of Nigeria. *Journal of Applied Geology and Geophysics*, 5(1), 37-45.
- Idri-Nda, A., Abubakar, S.I., Waziri, S.H., Dadi, M. I. and Jimada, A. M. (2015). Groundwater development in a mixed geological terrain: a case study of Niger state, Central Nigeria. *Water Resources Management VIII*, 196(1743-3541), 77-87. doi:10.2495/WRM150071
- Joshua, E.O., Layade, G O., Akinboboye, Y. B. and Adeyemi, S. A. (2017). Magnetic mineral exploration using ground magnetic survey data of Tajimi Area, Lokoja. *Global Journal of Pure and Applied Science*, 23, 301-310. doi:https://dx.doi.org/10.4314/gipas.v23i2.10
- Kayode, O., Oladele, S. and Salami, A. (2016). Geophysical Investigation of Banded Iron Ore Mineralisation at Ero, North-Central Nigeria. *RMZ-M&G*, 63, 109-118.
- Kheiralla, K. M., Mohamme-Ali, M. A., Abdelgalil, M. Y., Mohammed, N. E. and Boutsis, G. (2015). Integrated ERT and magnetic surveys in a mineralisation zone in Erkowit-Red Sea State-Sudan. *Journal of Engineering Research and Application*, 5(1(part5)), 9-17.
- Les, P. B., Berhe, G. and Jan, R. (2000). *Interpretation of low latitude magnetic anomaly*. Ethopia: Geological Survey of Norway.
- Loke, M. (2004). *2-D and 3-D electrical imaging surveys*. Retrieved from www.geoelectrical.com
- Lyatsky, H. (2010). *Magnetic and Gravity Methods in Mineral Exploration: the value of well-rounded geophysical skills*. Canadian Society of Exploration Geophysics.
- Mbonimpa, A.B., Barifaijo, E. and Tiberindwa, J.V. (2007, June). The potential for gold mineralisation in the greenschist belt of Busia district, South Eastern Uganda. *African Journals of Science and Technology*, 8(1), 116-134.
- McCurry, p. (1989). A general review of the geology of the precambrian to lower paleozoic rocks of northern Nigeria. In C. Kogbe, *Geology of Nigeria 2nd Edition* (pp. 13-37). Jos: Rock view (Nigeria) Limited.
- Mosaad, A., Shulin, S., Wei, Q., Abdou, D. B., Dusabemariya, C. and Yan, Z. (2020). Geoelectrical Tomography data processing and interpretation for Pb-Zn-Ag mineral

- exploration in Nash, Canada. *E3S Web of Conferences* 168.00003(2020). EDP Sciences.
- Nabighian, M. N., Grauch, V. J. S., Hansen, R. O., Lafehr, T. R., Li, Y., Peirce, J. W., Phillips, J. D and Rude, M. E. (2005). The historical development of the magnetic method in exploration. *Society of exploration geophysicist*, 70(6), 33-61.
- Obaje, N. G. (2009). Geology and Mineral Resources of Nigeria. In P. N. Obaje, *Lecture Notes in Earth Sciences* (p. 14). Keffi, Nasarawa: Springer Dordrecht Heidelberg London New York.
- Oyawoye, M. O. (1972). The Basement Complex of Nigeria. In A. J. Dessauvague and Whiteman, *African Geology* (pp. 67-98). Ibadan University Press.
- Peter, W. K. (2019). Gold: Relationship between magnetic anomalies and epigenetic gold mineralisation in the Victory-Defiance Area, Western Australia. *ASEG*, 283-296. doi:10.1071/ASEGSpec07_20
- Philip, K., Micheal, B. and Ian, H. (2002). *An Introduction to Geophysical Exploration*. Berlin, Germany: Blackwell Sciences.
- Rafiu Abdulwaheed & Abu Mallam. (2014, December). Investigating Groundwater Contamination Using Vertical Electrical Sounding and Physio-Chemical Analysis around Anguwan Jukpa Municipal Solid Waste, Minna, North-Central, Nigeria. *Journal of Applied Geology and Geophysics*, 2(6), 06-10.
- Ravindran, A. A. (2012, June). Evaluation of Iron ore deposits in Elayiran Pannai, Suttur Taluk, Virudhunagar District and Tamilnadu Using 2D Electrical Resistivity Imaging. *JASEM*, 16(2)171-173.
- Reynolds, J. M. (2011). *An introduction to Applied and Environmental Geophysics* (2nd ed.). New Delhi: Wiley-Blackwell.
- Rowland, A. A. (2019, March). Interpretation of High Resolution Aeromagnetic Data for Hydrocarbon Potentials over Parts of Nasarawa and Environs, North Central Nigeria. *World Journal of Applied Physics*, 4(1), 1-11.
- Saeed, K. A, Gbolan, H. N., Faramarz, D. A. and Maysam, A. (2015). Application of Magnetometry, Electrical Resistivity and Induced Polarisation for Exploration of Polymetal deposits, a case study of Halab Dandi, Zanjan, Iran. *2nd International conference on Advances in Engineering Sciences and Applied Mathematics*. Istanbul.
- Sedara, S. O., Alabi, O. O. and Akinwande, D. D. (2016). Depth estimation of mineral deposit using Magnetic methods in Oduduwa University, Ipetumodu, Southwestern Nigeria. *FUTA Journal of Research in Sciences*, 12(2), 325-333.

- Sultan, A. S., Salah, A. M., Fernando, M. and Ahmed, S. (2009, September 8). Geophysical exploration for gold and associated minerals, case study, Wadi El Beida area, South Eastern Desert, Egypt. *Journals of Geophysics and Engineering*, 345-356. doi:10.1088/1742-2132/6/4/002
- Telford, W.M., Geldart, L.P., Sheriff, R.E. (1990). *Applied Geophysics*. New York: Cambridge University press.
- Tigistu Haile & Alemayehu Ayele. (2014). Electrical Resistivity Tomography and Magnetic Surveys: Application for Building Site Characterisation at Gubre, Wolkite University Site, Western Ethiopia. *Ethiopia Journal of Sciences*, 37(1), 13-30.
- Truswell, J. F. and Cope, R. N. (1963). Parts of Niger and Zaria provinces, Northern Nigeria. *Geological Survey, Nigeria Bull 29*, pp. 1-104.